

RIA-77-U1211

TECHNICAL  
LIBRARY

Structural Analysis Programs Applied  
to Warhead Impact Problems

by  
W. J. Stronge  
and  
J. C. Schulz  
*Research Department*

DTIC QUALITY INSPECTED 2

NOVEMBER 1977

Approved for public release; distribution unlimited.

19970723 189

Naval Weapons Center

CHINA LAKE, CALIFORNIA 93555



# Naval Weapons Center

AN ACTIVITY OF THE NAVAL MATERIAL COMMAND

## FOREWORD

The research described in this report is concerned with the use of finite element programs to solve impact-type problems. It is part of a continuing effort to strengthen our capabilities in the area of warhead structural analysis. This work was performed during fiscal year 1977 and authorized by AIRTASK WF32-353-501.

This report is released at the working level. Because of the continuing nature of the warhead research and development program, refinements and modifications may later be made in this study.

Approved by  
E. B. ROYCE, Head  
Research Department  
1 November 1977

Under authority of  
W. L. HARRIS, JR.  
RAdm., U.S. Navy  
Commander

Released for publication by  
R. M. HILLYER  
Technical Director (Acting)

NWC Technical Publication 5981

Published by.....Technical Information Department  
Collation.....Cover, 22 leaves  
First printing.....160 unnumbered copies

UNCLASSIFIED

SECURITY CLASSIFICATION OF THIS PAGE (When Data Entered)

REPORT DOCUMENTATION PAGE		READ INSTRUCTIONS BEFORE COMPLETING FORM
1. REPORT NUMBER NWC TP 5981	2. GOVT ACCESSION NO.	3. RECIPIENT'S CATALOG NUMBER
4. TITLE (and Subtitle) STRUCTURAL ANALYSIS PROGRAMS APPLIED TO WARHEAD IMPACT PROBLEMS		5. TYPE OF REPORT & PERIOD COVERED Final report
7. AUTHOR(s) W. J. Stronge, J. C. Schulz		6. PERFORMING ORG. REPORT NUMBER
9. PERFORMING ORGANIZATION NAME AND ADDRESS Naval Weapons Center China Lake, CA 93555		10. PROGRAM ELEMENT, PROJECT, TASK AREA & WORK UNIT NUMBERS AIRTASK WF32-353-501
11. CONTROLLING OFFICE NAME AND ADDRESS Naval Weapons Center China Lake, CA 93555		12. REPORT DATE November 1977
14. MONITORING AGENCY NAME & ADDRESS (if different from Controlling Office)		13. NUMBER OF PAGES 42
		15. SECURITY CLASS. (of this report) UNCLASSIFIED
		15a. DECLASSIFICATION/DOWNGRADING SCHEDULE
16. DISTRIBUTION STATEMENT (of this Report)  Approved for public release; distribution unlimited.		
17. DISTRIBUTION STATEMENT (of the abstract entered in Block 20, if different from Report)		
18. SUPPLEMENTARY NOTES		
19. KEY WORDS (Continue on reverse side if necessary and identify by block number) Finite elements NASTRAN Impact ADINA Warheads SAP IV Structural analysis HONDO		
20. ABSTRACT (Continue on reverse side if necessary and identify by block number)  See back of form.		

UNCLASSIFIED

SECURITY CLASSIFICATION OF THIS PAGE(When Data Entered)

*Structural Analysis Programs Applied to Warhead Impact Problems* by W. J. Stronge and J. C. Schulz. China Lake, Calif., Naval Weapons Center, November 1977. 42 pp. (NWC TP 5981, publication UNCLASSIFIED.)

(U) This report is concerned with the application of general purpose finite element structural analysis programs to warhead design work. The capabilities of a number of linear and nonlinear programs including NASTRAN, SAP IV, ADINA, and HONDO are described. These programs are used to solve a number of impact-type problems ranging in complexity from a simple one-dimensional rod to a conical steel warhead filled with explosive. The results are compared on the basis of accuracy, time and cost, ease of learning, and ease of use.

UNCLASSIFIED

SECURITY CLASSIFICATION OF THIS PAGE(When Data Entered)

## INTRODUCTION

Warheads intended to penetrate a target and detonate within it must be able to withstand the shock loading resulting from impact. In particular, the warhead case, the explosive, and the fuze must each remain intact and functional. The rational design of such warheads requires a knowledge of the transient stresses, displacements, and/or accelerations produced. These can then be compared with appropriate damage criteria to determine the survivability of a particular configuration. Experimental data on these variables is difficult to obtain. Structural analysis programs employing the finite element method provide the designer with an attractive alternative method of obtaining this information.

Although the finite element method has been in use for a number of years, it is only comparatively recently that codes have been developed that bring the solution of large-scale transient problems, and particularly nonlinear problems, to the threshold of economic feasibility.<sup>1</sup> In the finite element method, the body to be analyzed, which may possess an infinite number of degrees of freedom, is represented by an approximate model consisting of a number of idealized structural elements connected at specified nodal points, and possessing only a finite and relatively small number of degrees of freedom. The response of this model to the applied loads or displacements is then determined. The accuracy of the solution obtained depends primarily on the number of degrees of freedom in the model and, in the case of dynamic problems, on the time step used in the numerical integration.

The limitations of structural analysis programs for design work are primarily those of cost and time. Impact problems, because of the high stress gradients and associated steep wave fronts involved, require models with many degrees of freedom and small time steps to obtain accurate results. The cost of a finite element solution can be expected to increase approximately as the square of the number of degrees of freedom and directly as the number of time steps used. Not only does the computer cost become large for impact problems, but the time in man-hours for the construction of models and the input of data also becomes large.

---

<sup>1</sup> *Finite Element Analysis of Transient Nonlinear Structural Behavior*, T. Belytschko, et al, eds. Amer. Soc. Mech. Eng., AMD-Vol. 14, 1975.

In addition, the amount of output data generated and the time required for its interpretation increase significantly.

In this report a number of linear and nonlinear structural analysis programs are described and then applied to the solution of impact-type problems ranging in complexity from a simple one-dimensional rod to a conical warhead filled with explosive. The results provide information as to the suitability of finite element programs for warhead design work. The various programs are compared on the basis of accuracy, time and cost, ease of learning, and ease of use. Recommendations as to which programs appear most useful for different problems are offered.

#### DESCRIPTION OF PROGRAMS

A wide variety of linear and nonlinear structural analysis programs have been developed and are being used in government and industry at the present time. Some of these are proprietary, others are available on a lease basis, and still others can be obtained free or at nominal cost. The particular programs looked at in this study, most of which fall into the last category, are described in the following paragraphs. In addition, some features of the various programs are compared in Table 1.

NASTRAN is probably the most widely used and continuously developed program available for linear analysis. Impact problems can be analyzed by either the transient or modal techniques. A full range of element types is available. NASTRAN has excellent routines for generating structure plots and plots of stresses and other output quantities. However, a lack of grid and element data generation routines makes problem input time consuming. Initial training in the use of this program is required because of the large number of options available and a poor method of indexing in the user's manual.

SAP IV is another widely used linear analysis program. Its range of features and capabilities is not quite as broad as in the case of NASTRAN. On the other hand, it is simpler to learn and easier to use, especially for the type of problems considered in this study. SAP IV has convenient grid and element data generation routines that reduce the amount of work involved in problem input.

SHELL SHOCK is yet another linear program capable of handling transient problems. It offers a choice between implicit and explicit time integration techniques. Three types of structural elements are generated internally: beams, shells, and solids of revolution. Although restricted to axisymmetric structures, the program can treat nonaxisymmetric loadings (as might occur during the oblique impact of warheads). The loading is broken down into a series of Fourier harmonics, and the response to each harmonic is determined separately.

TABLE 1. Comparison of Programs

Program	Analysis type	Geometry	Elements	Materials		Available on NWC	UNIVAC 1110													
				3-D	Plane stress	Axisymmetric	3-D solid	2-D solid	Plate-shell	Membrane	Beam	Shear panel	Elastic	Viscoelastic	Fluid	Solid	Crushable foam	Rubber-like	Plot routines	Data generation
NASTRAN	X	X	X	X	X	X	X	X	X	X	X	X	X	X	X	X	X	X	X	X
SAP IV	X	X	X	X	X	X	X	X	X	X	X	X	X	X	X	X	X	X	X	X
SHELL SHOCK				X																
NONSAP	X	X	X	X	X	X	X	X	X	X	X	X	X	X	X	X	X	X	X	X
ADINA	X	X	X	X	X	X	X	X	X	X	X	X	X	X	X	X	X	X	X	X
HONDO					X															
MARC	X	X	X	X	X	X	X	X	X	X	X	X	X	X	X	X	X	X	X	X
TOODY-IIA																				

NONSAP is a nonlinear program capable of solving impact problems by either modal superposition or direct integration. Both geometric and material nonlinearities (i.e., large deformations and plasticity) can be handled. However, the nonlinear capabilities are limited to axisymmetric configurations subjected to axisymmetric loads. Like SAP IV, to which it is similar in format, NONSAP is easy to use. Currently, the dynamic capabilities of the program are not functional on the NWC UNIVAC 1110, so only static analyses can be run. This program is not supported by the developers.

ADINA is a follow-on program to NONSAP that has been fully implemented on the UNIVAC machine. ADINA offers additional material models, and its nonlinear capabilities extend to general three-dimensional problems.

HONDO can be used to calculate the large deformation elastic, or inelastic transient response of two-dimensional solids. Time integrations are performed using an explicit central difference method. Solutions are obtained entirely in core. This makes the program very fast but restricts the model size. Eight material subroutines are available including elastic, elastic-plastic, and viscoelastic behavior. Though somewhat limited as to the class of problems it can solve, HONDO is by far the simplest of the programs to use.

MARC has a reputation for the broadest capability of nonlinear analysis and also the slowest execution time. It has a full complement of modern elements and material representations. It can treat nonaxisymmetric, nonlinear transient deformations. There are excellent pre and post processors including plotting that make the program handy to use. It seems to be easy to learn. MARC is a proprietary program obtained on a lease basis.

TOODY-IIA is a two-dimensional Lagrangian hydrocode suitable for computing wave propagation in two dimensions in rectangular or cylindrical coordinates. The code is based on the conventional finite difference analogs to the nonlinear Lagrangian equations of motion. TOODY-IIA is applicable over a wide range of conditions including such material properties as elastic-plastic, crushable foams, deformable solids, explosives, and fluids. The geometry capability is very general and colliding objects can be modeled. This code provides a sliding interface option.

#### TRANSIENT LOADING PROBLEMS

##### ONE-DIMENSIONAL ROD

The first problem considered is that of a one-dimensional, elastic rod built in at one end and loaded at the other end with a half sine

pressure pulse. The rod has unit properties, while the pressure pulse is of unit maximum intensity and is applied over a period of time such that the length of the pulse is one-tenth the length of the rod. The problem geometry is shown in Figure 1. This problem is included because it is relatively simple and has a known analytic solution and not because it is a reasonable representation of an impacting warhead.

The problem was solved using NASTRAN and SAP IV. For modeling purposes the rod was divided into 20 truss-type elements and an integration time step chosen such that 100 steps were required for the pressure pulse to travel the length of the rod and return to the free end. Centerline displacements along the length of the rod are plotted for five successive times in Figure 2. NASTRAN and SAP IV results are shown along with the exact solution. A zone of constant displacement is created behind the pressure pulse as it travels down the rod. After the pulse is reflected from the built-in end, this displacement is removed as the pulse travels back to the free end. Under the pressure pulse itself, the displacement varies sinusoidally from zero to its constant value.

Except for the presence of oscillations about the true solution, both programs provide a reasonably good gross representation of the zones of zero and constant displacement in the rod. On the other hand, the finite element solutions do not accurately describe the displacement under the pulse itself. Oscillations, such as observed here, are typical of finite element solutions to transient problems, and in more complex situations they sometimes render the interpretation of results difficult. It would appear that the amplitude of the oscillations is slightly less in the SAP IV solution (20 elements), possibly due to a larger artificial viscosity effect from the Wilson  $\theta$  method of integration used in that program.

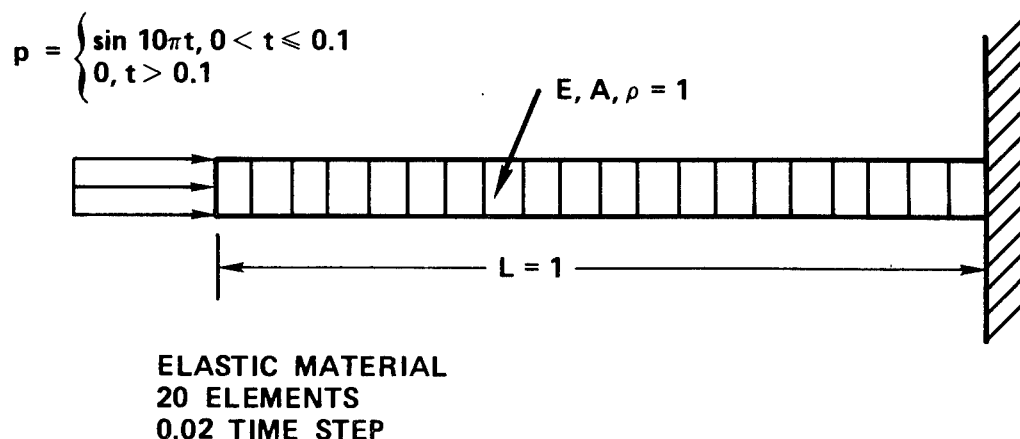


FIGURE 1. One-Dimensional Rod Geometry.

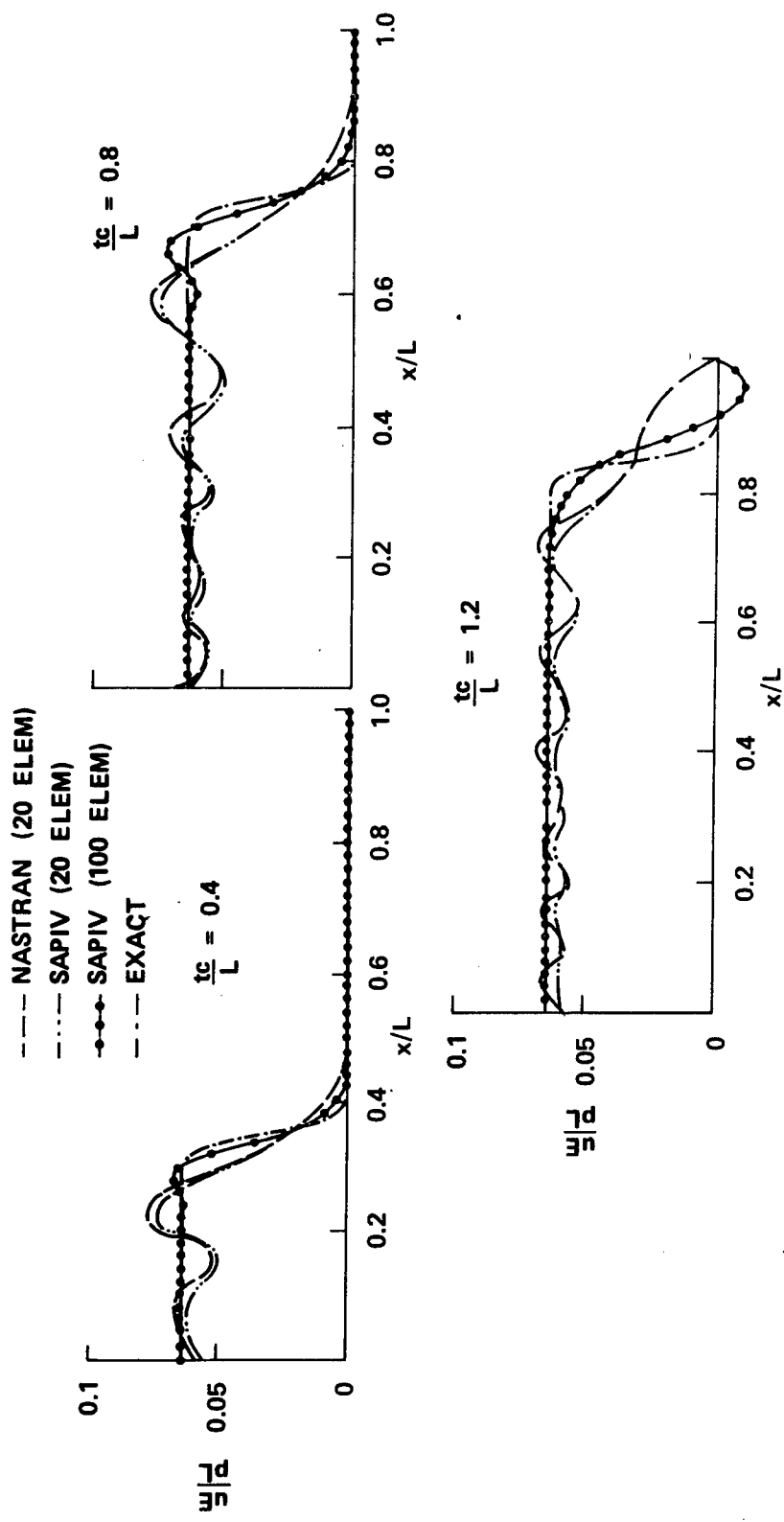


FIGURE 2. One-Dimensional Elastic Rod, Axial Displacement Versus Axial Distance From Free End at Selected Times.

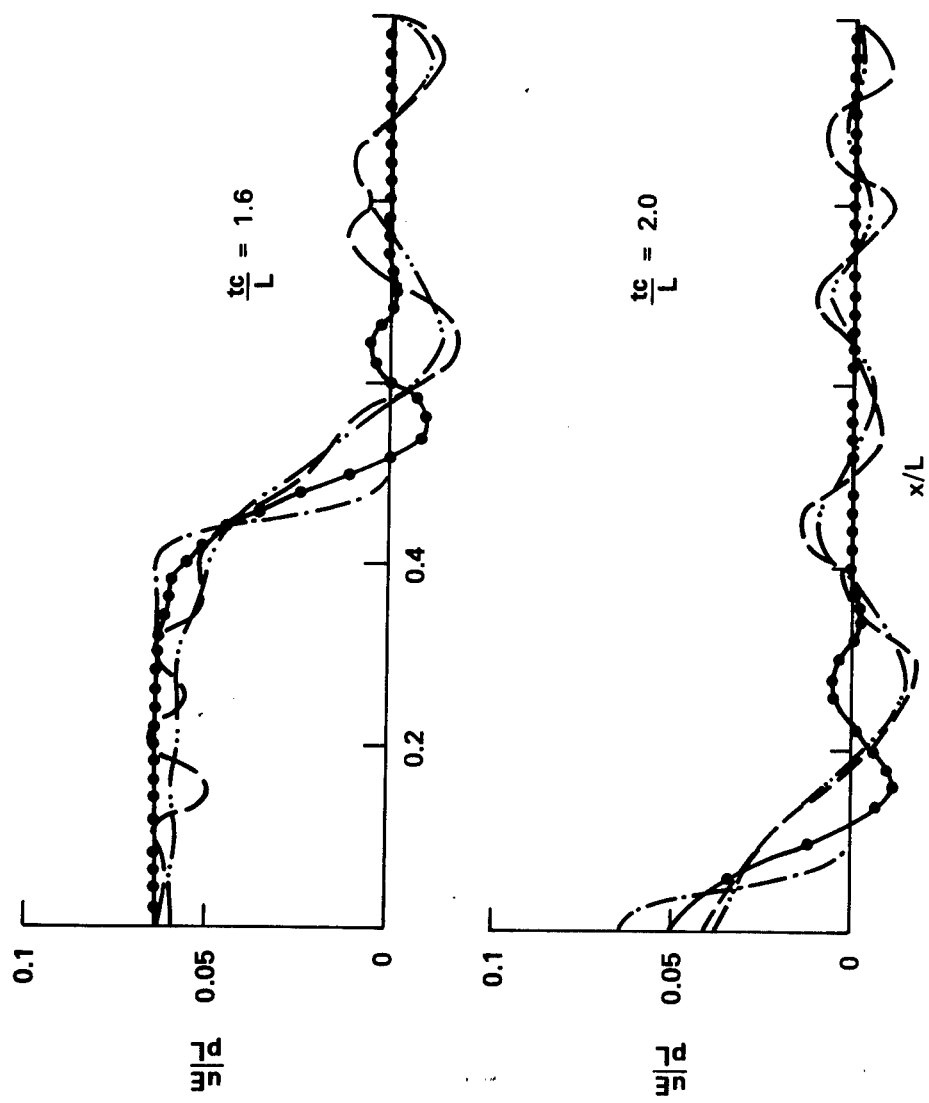


FIGURE 2. (Contd.)

The accuracy of a finite element solution can be improved through the use of more elements and smaller integration time steps. Also shown in Figure 2 are SAP IV results obtained using a model consisting of 100 elements integrated over 200 time steps. It is obvious that the oscillations about the true solution in the zones of zero and constant displacement have been substantially reduced. However, the accuracy under the pulse itself is still not very good, especially at later times.

In actual design work the shape of the applied pressure pulse would not be known with any degree of precision, and the exact displacement under the pulse would not be of interest. Hence, the solution given here would be satisfactory. If greater accuracy were desired, however, a finer model consisting of about 1,000 elements could be used. For this simple one-dimensional problem the additional run cost would be insignificant. In the case of a two- or three-dimensional problem, however, a model with the equivalent of 1,000 elements in two or three directions would be extremely expensive in terms of computer time.

A similar problem was solved for a material with nonlinear material properties. In particular, bilinear behavior was assumed corresponding to an elastic-plastic material with linear strain hardening. The moduli in the two linear regions were chosen so as to make the plastic wave speed half the elastic wave speed. The rod, again, had unit properties and was built-in at one end. In this case, however, the other end was loaded with a step pressure equal to twice the yield stress.

This problem was solved using ADINA and HONDO. For the ADINA solution, the rod was modeled with 100 beam elements. A time step of .01 was used. Since HONDO does not have one-dimensional elements in its library, it was necessary to use a two-dimensional representation consisting of a single row of 100 axisymmetric elements down the length of the rod. To minimize transverse inertia effects, the diameter of the rod was made small compared to its length ( $D/L = .01$ ). It was not necessary in this case to select an integration time step since HONDO automatically computes an appropriate step such as to ensure stability of the numerical integration.

The results are shown in Figure 3, which is a series of plots of axial stress versus axial distance from the free end at selected times. The exact solution, which is characterized by the presence of elastic and/or plastic wave fronts traveling along the rod, is also shown. Agreement between HONDO and the exact solution is quite good except in the immediate vicinity of the discontinuities at the wave fronts, which any finite element program would have difficulty representing. The ADINA solution, however, oscillates wildly around the exact solution. These oscillations only occur in the region of plastic behavior. ADINA results are plotted for the first time step only because they get worse at later times. It is not clear whether these oscillations are due to an error in the version of the program implemented at NWC, or whether

they are inherent in the program itself, perhaps resulting from the implicit integration technique used. A new version of ADINA is scheduled for release soon. This new version will have, among other features, an explicit time integration option. It would be of interest to rerun this problem using the new version to see if improved results are obtained.

#### ROD WITH TRANSVERSE INERTIA

In the one-dimensional rod idealization, the effects of transverse inertia of the material are neglected: Inclusion of these effects by means of the Pochhammer-Chree equations greatly complicates the problem. The shape of a wave front propagating down the rod no longer remains constant, but becomes degraded and dispersed due to the transfer of part of its energy into transverse vibration. Even for such a simple appearing problem as the application of a step pressure to the end of a semi-infinite circular cylinder, no satisfactory analytic solution exists. A formal solution to this problem as a sum of Fourier integrals has been obtained by Folk, et al.<sup>2</sup> These integrals cannot be evaluated by simple means, and Folk, et al, were forced to obtain asymptotic solutions which are approximately valid only at large distances from the loaded end.

Noting the lack of analytical results for cylinders near the point of application of a load, Bertholf<sup>3</sup> employed a finite difference technique to solve the problem of a one-diameter-long cylinder subjected to a step pressure at one end and rigid-lubricated at the other. Because his solution appears to be quite accurate, the same problem was run in this study using NASTRAN and SAP IV and the results compared. A 300-element model of the cylinder was used. The cylinder geometry and properties, as well as the finite element representation, are shown in Figure 4.

Plots of axial strain at the free surface of the cylinder versus axial distance from the loaded end for four successive nondimensional times are given in Figure 5. The Bertholf solution, the two finite element solutions, and also the one-dimensional rod solution are shown. It can be seen that the two finite element solutions agree quite closely with one another and are in reasonably good overall agreement with the Bertholf solution. However, the fine points of the Bertholf solution (in particular, the undulations behind the front of the wave) are not

---

<sup>2</sup> R. Folk, et al. "Elastic Strain Produced by Sudden Application of Pressure to One End of a Cylindrical Bar," *Acoust. Soc. Amer., J.*, Vol. 30 (1958), p. 552.

<sup>3</sup> L. D. Bertholf. "Numerical Solution for Two-Dimensional Elastic Wave Propagation in Finite Bars," *J. Appl. Mech.*, Vol. 34, Trans., ASME (Vol. 89), Series E (1967), p. 725.

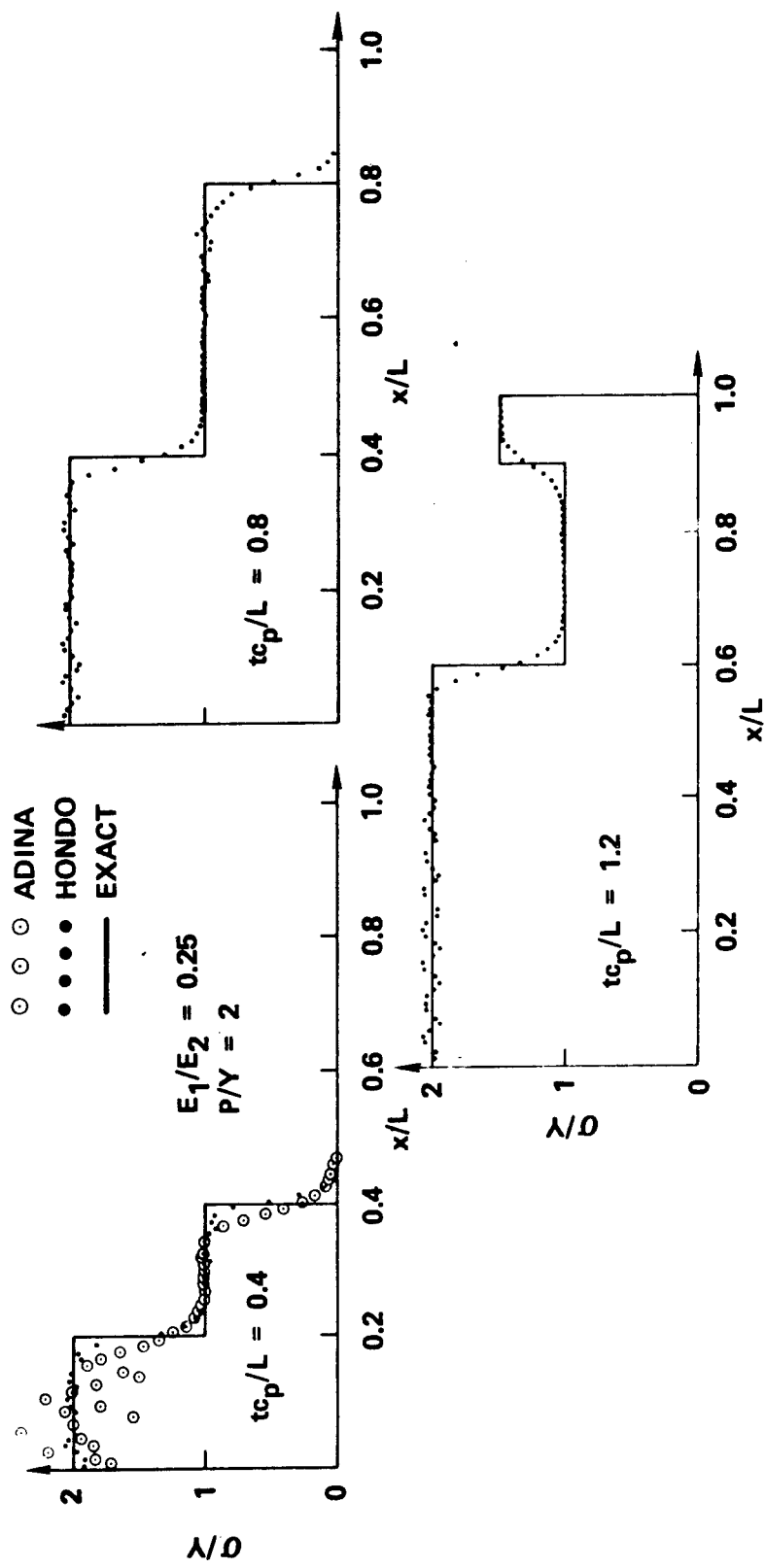


FIGURE 3. One-Dimensional Elastic-Plastic Rod, Axial Stress Versus Distance From the Free End at Selected Times.

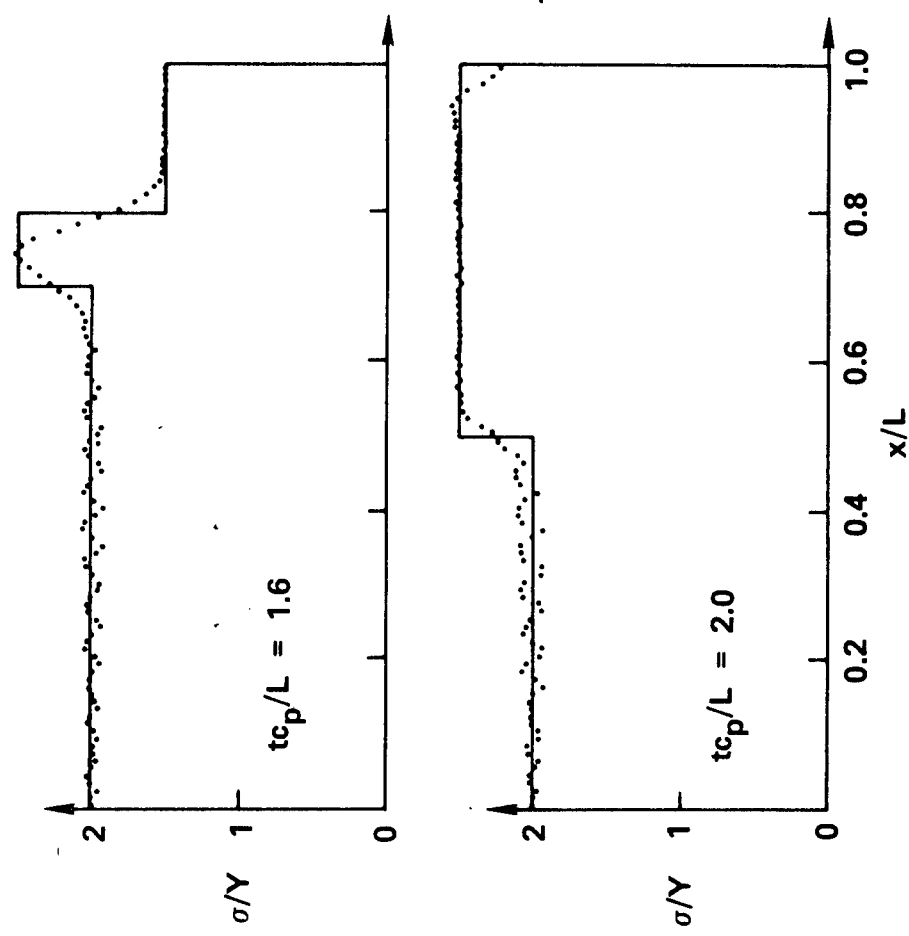


FIGURE 3. (Contd.)

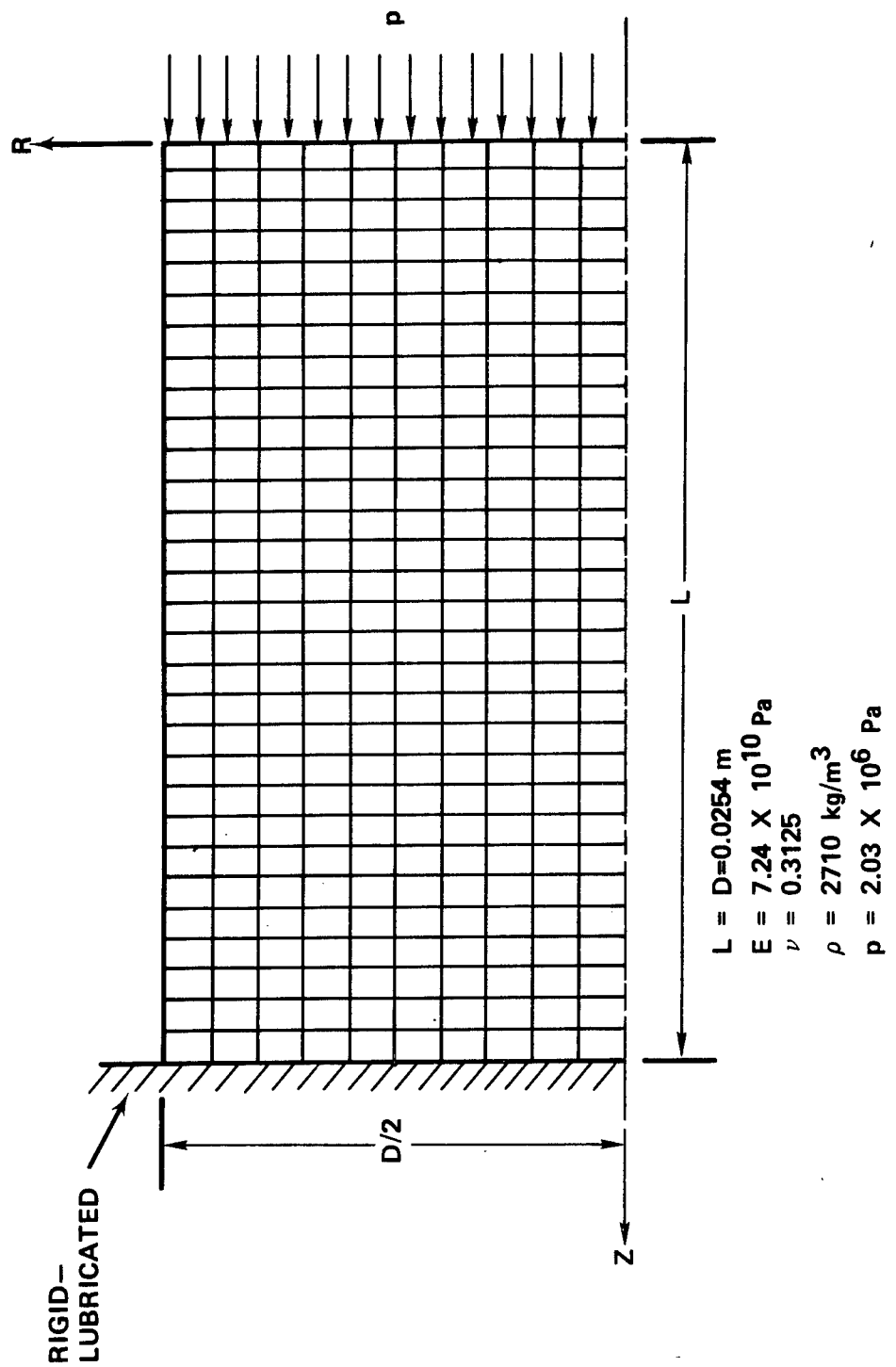


FIGURE 4. Finite Element Model of Bertholf Cylinder, Elastic.

picked up by either finite element solution. The NASTRAN solution is in slightly better agreement with the Bertholf solution, especially in its representation of the steepness of the wave front. The SAP IV solution is more smoothed out and less detailed, again perhaps due to a larger damping effect from the Wilson  $\theta$  method of integration. It is possible that the Bertholf solution, being itself an approximate solution, is no more accurate or correct than the others. Assuming that it is, however, it follows that a considerably more refined finite element model is required to approximate the Bertholf results. It should be noted that the one-dimensional rod solution becomes an increasingly poor description of the actual strain behavior as time increases.

Bertholf and Karnes<sup>4</sup> give a finite difference solution to a similar problem, this time involving a nonlinear material. Specifically, the problem is that of the longitudinal impact of two elastic-plastic cylinders. The cylinders were 0.0635 meters long, 0.0318 meters in diameter, and were made of 6061-T6 aluminum. The elastic-plastic material was assumed to follow von Mises' yield criterion and have isotropic strain hardening. An approach velocity of the two cylinders of 100 m/s was considered. Bertholf and Karnes also obtained experimental results with which to compare their theoretical solution.

This problem was solved in the present study using HONDO. By symmetry, only one of the cylinders was considered. A model consisting of six layers of axisymmetric elements with 25 elements in each layer was used. The cylinder was given an initial longitudinal velocity of 50 m/s. Points at the impact end were constrained from movement in the longitudinal direction, but were allowed to move freely in the radial direction (rigid-lubricated). The geometry and properties are shown in Figure 6.

Results in the form of plots of axial strain at the surface versus time at distances  $z = R/12$ ,  $R$  and  $2R$  from the impact end are given in Figure 7. The numerical and experimental results of Bertholf and Karnes are also shown. Agreement between theory and experiment appears to be quite good considering the experimental difficulties involved. The Bertholf and Karnes solution is in better agreement with experiment than the HONDO solution, especially at larger times. This is to be expected since the Bertholf and Karnes solution utilizes a much finer mesh (3,600 grid points as opposed to 182 for HONDO). However, it should be noted that the Bertholf and Karnes solution required about three hours on a CDC 3600 computer compared to about one minute on the UNIVAC 1110 for the HONDO solution. The greater error in the HONDO solution, therefore, must be weighed against the fact that it cost virtually nothing to obtain.

---

<sup>4</sup> L. D. Bertholf and C. H. Karnes. "Axisymmetric Elastic-Plastic Wave Propagation in 6061-T6 Aluminum Bars of Finite Length," *J. Appl. Mech.*, Vol. 36, Trans., ASME, Vol. 91, Series E (1969), p. 533.

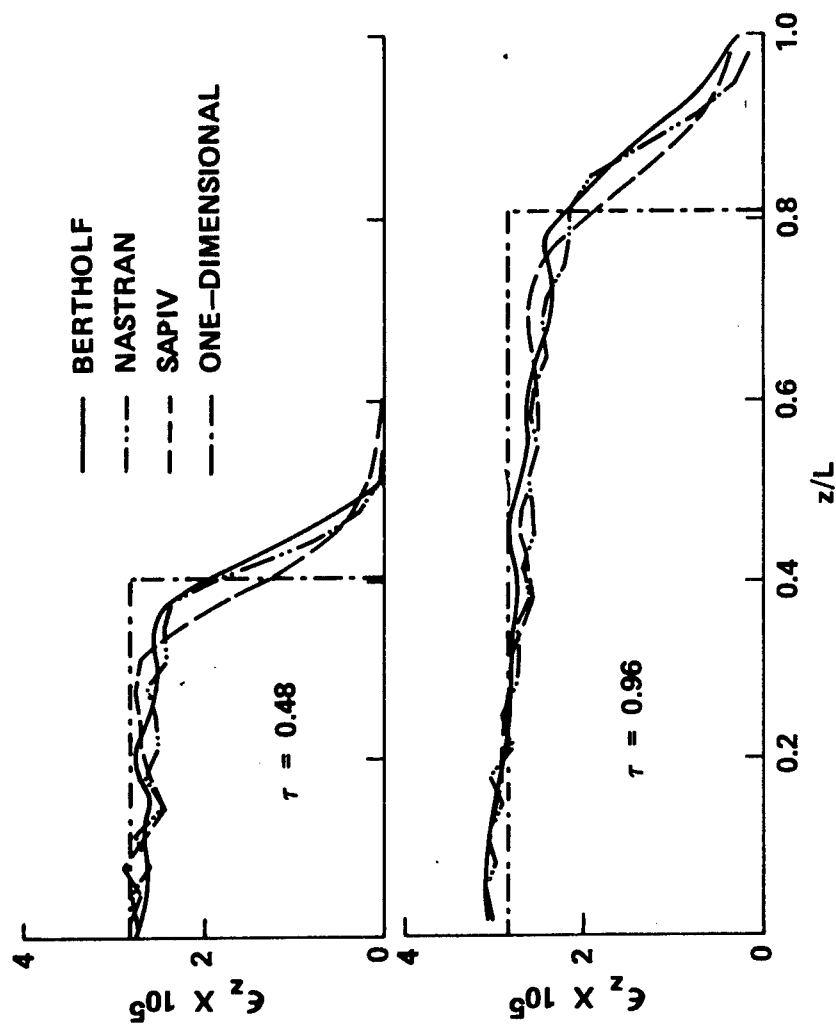


FIGURE 5. Elastic Rod With Transverse Inertia, Axial Strain at Free Surface Versus Axial Distance.

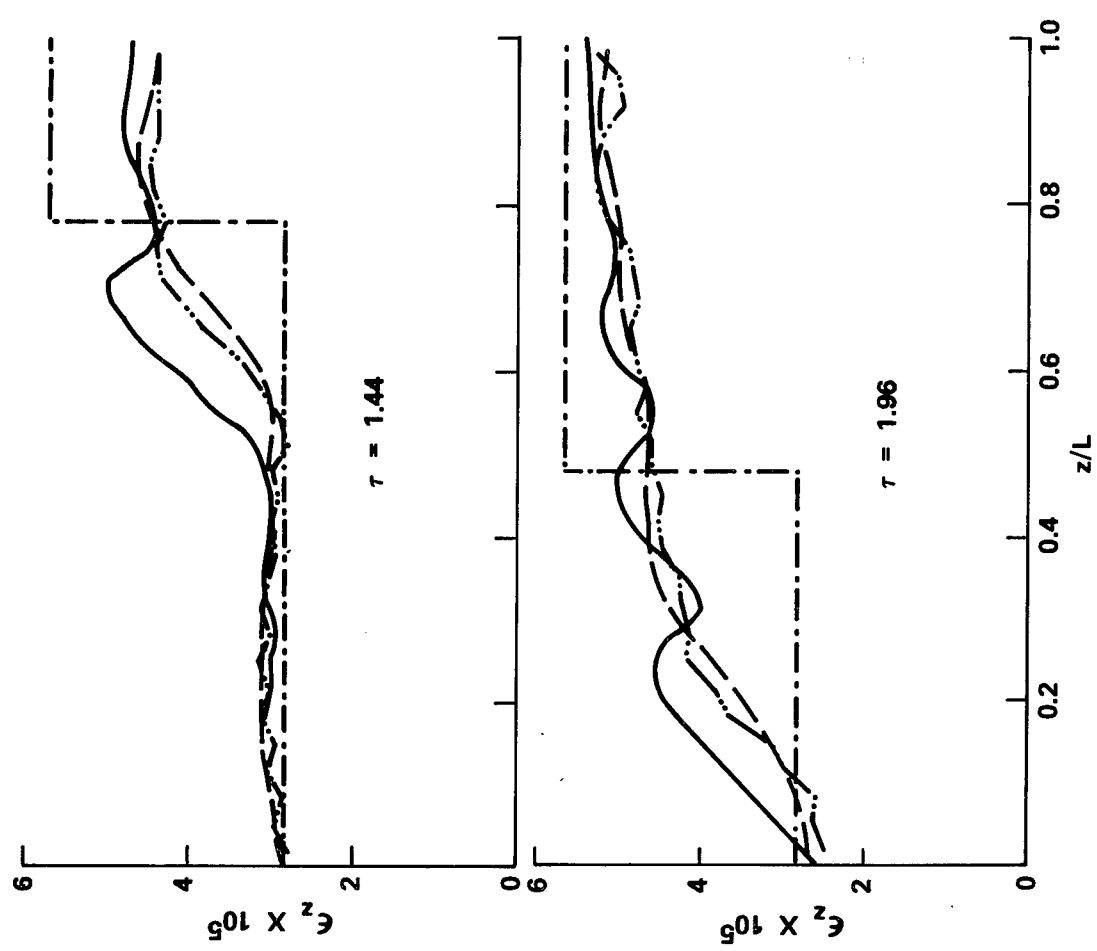


FIGURE 5. (Contd.)

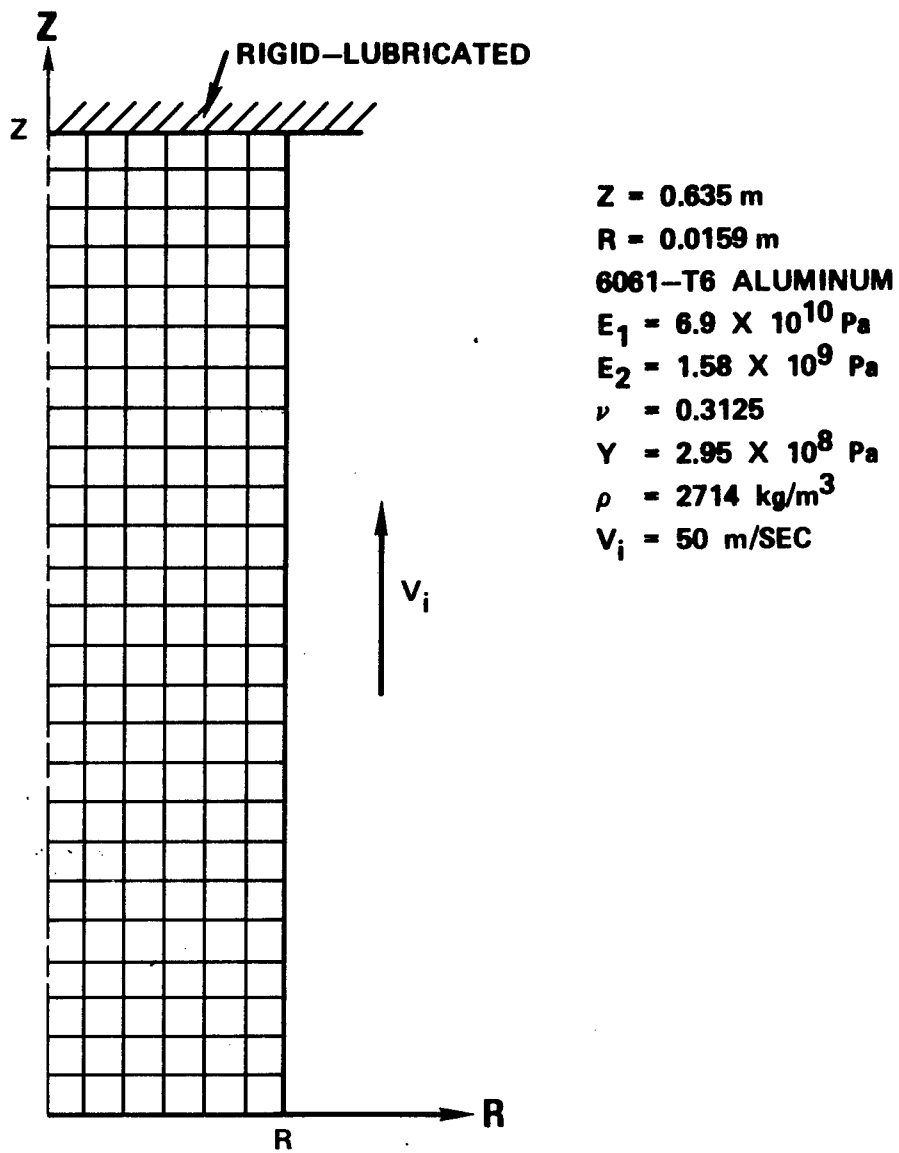


FIGURE 6. Geometry and Properties of Bertholf-Karnes Elastic, Plastic Cylinder.

#### EXPLOSIVE-FILLED STEEL CYLINDER

Comparison of Codes. Warhead impact with a hard target at normal obliquity has been investigated with the model shown in Figure 8. A 0.1-meter-long cylinder, 0.1 meter in diameter is composed of a thin steel case filled with explosive. The case is assumed to be elastic for stress states within the von Mises yield condition and have linear kinematic strain hardening for stress states satisfying the yield criterion. The explosive is assumed to be a linear elastic material. Material properties

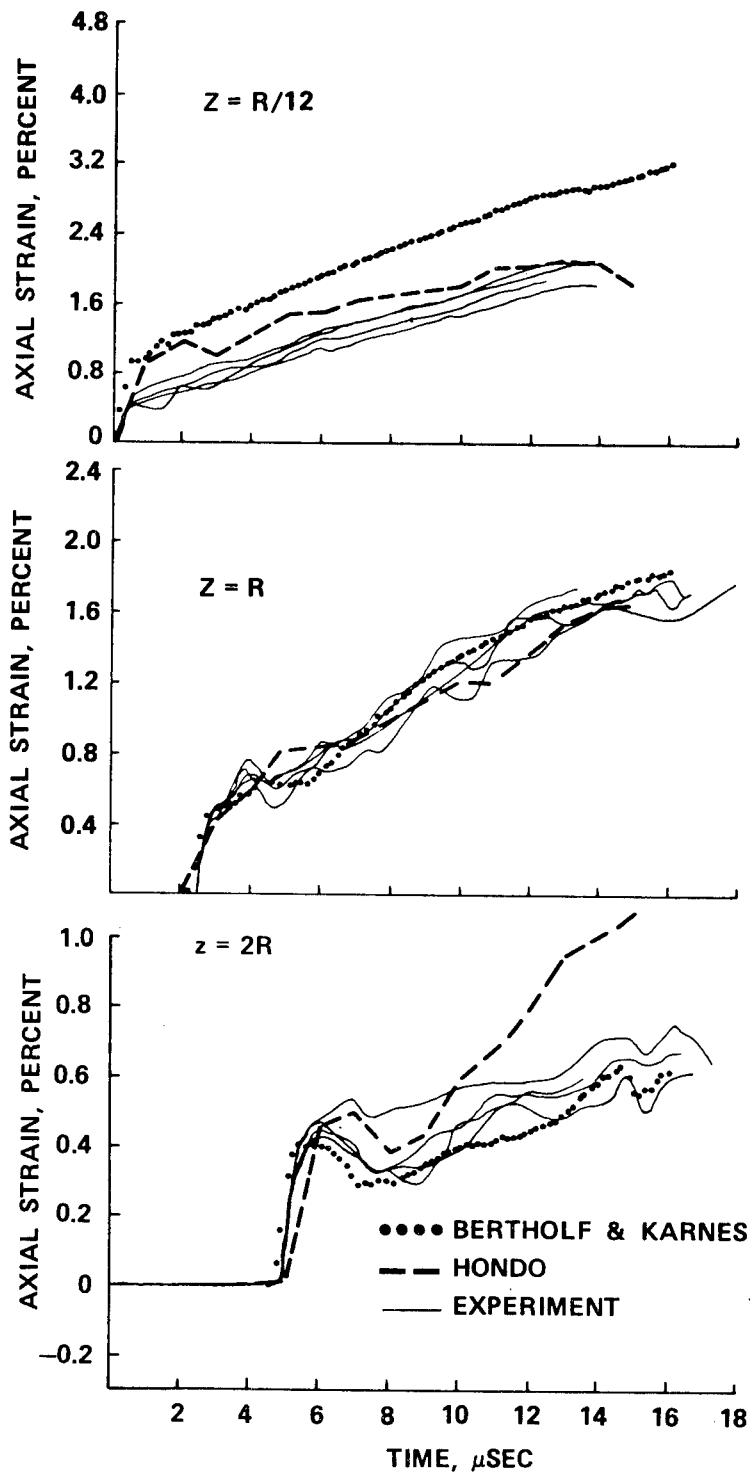


FIGURE 7. Elastic-Plastic Rod With Transverse Inertia, Axial Strain at Free Surface Versus Axial Distance.

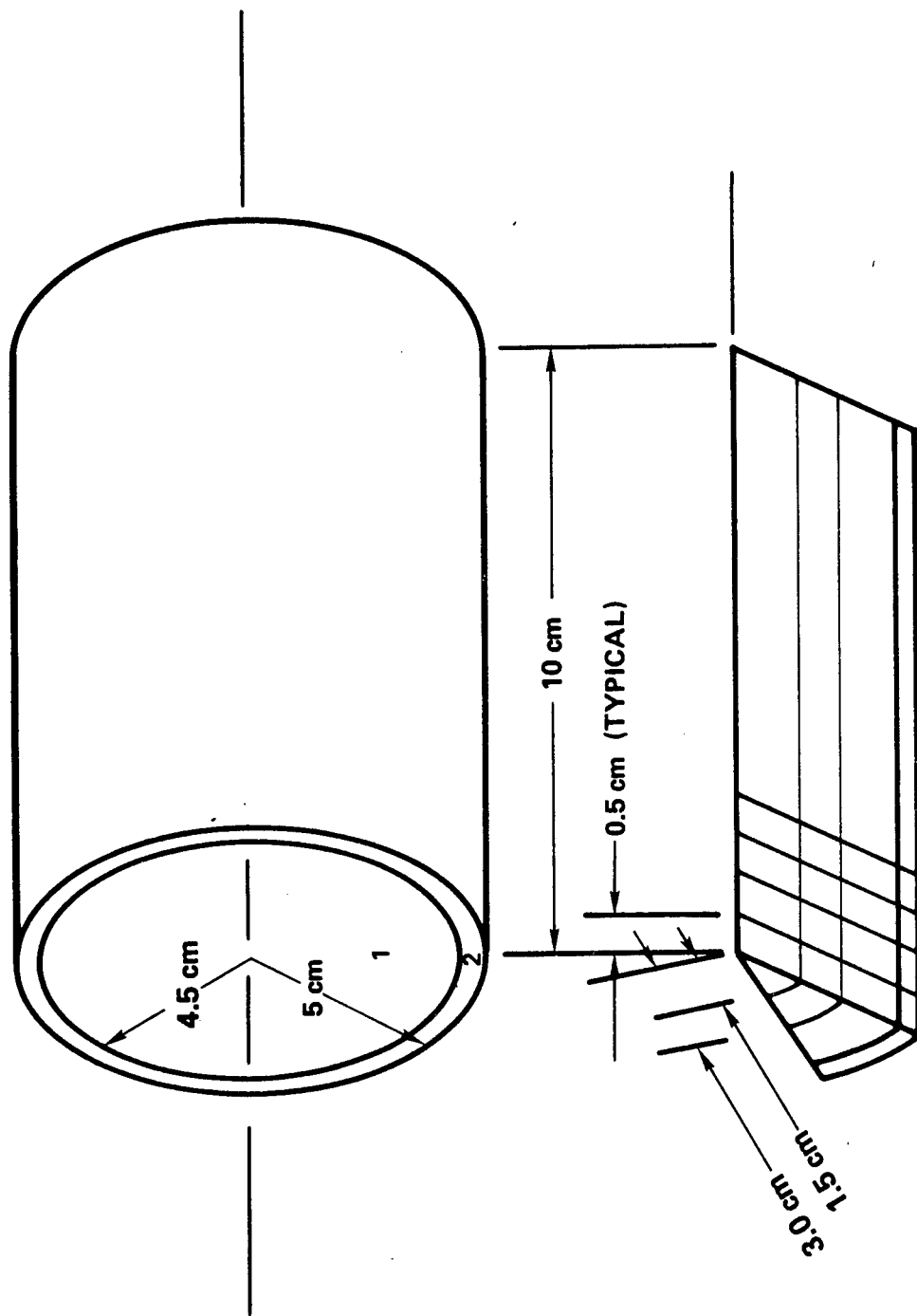


FIGURE 8. Finite Element Model of Cylinder.

used in this analysis are shown in Table 2. The failure stress for steel is the one-dimensional tensile yield stress while the explosive failure stress is the lowest pressure at which deflagration occurs. A coarse finite element model of this warhead configuration has been analyzed. The model uses three layers of axisymmetric elements for the explosive core and one layer for the case (see Figure 8).

TABLE 2. Cylinder Material Properties.

Material	Stress-strain constants		Density $\rho$ , Kg/m <sup>3</sup>	Wave speed m/sec	Failure- stress, Pa
	E, Pa	$\nu$			
Steel (elastic)	$2.0 \times 10^{11}$	0.3	7800	$C_r = 5060$	$6.9 \times 10^8$
Steel (plastic)	$2.0 \times 10^9$	0.3	7800	$C_r = 506$	--
PBX (expl) <sup>5</sup>	$6.9 \times 10^9$	0.34	1800	$C_1 = 2420$	$5.0 \times 10^8$

A half sine pressure pulse of 5  $\mu$ sec duration is applied to one end of the cylinder. Two loading cases with different pressure amplitudes have been defined in Table 3. Load 1 should impart a uniform 1 m/sec axial velocity to the end of the cylinder. The resultant stresses at the impacting end will be in the plastic range. Only those codes with the capability to analyze nonlinear material response (ADINA, HONDO and MARC) have been used for case 2.

TABLE 3. Pressure Amplitude.

Case	$P_1$ (explosive)	$P_2$ (case)
1	$4.32 \times 10^6$ Pa	$10.8 \times 10^8$ Pa
2	$39.46 \times 10^6$ Pa	$16.06 \times 10^8$ Pa

Axial displacements on the centerline and on the explosive-case interface have been calculated by the appropriate codes. These displacements are compared at 10, 20, and 30  $\mu$ sec after impact in Figures 9 and 10 for elastic and elastic-plastic deformations, respectively.

<sup>5</sup> Lawrence Livermore Laboratory. *Properties of Chemical Explosives and Explosive Simulants*, by B. M. Dobratz. University of California, July 31, 1974. (UCRL 51319, Rev. 1.)

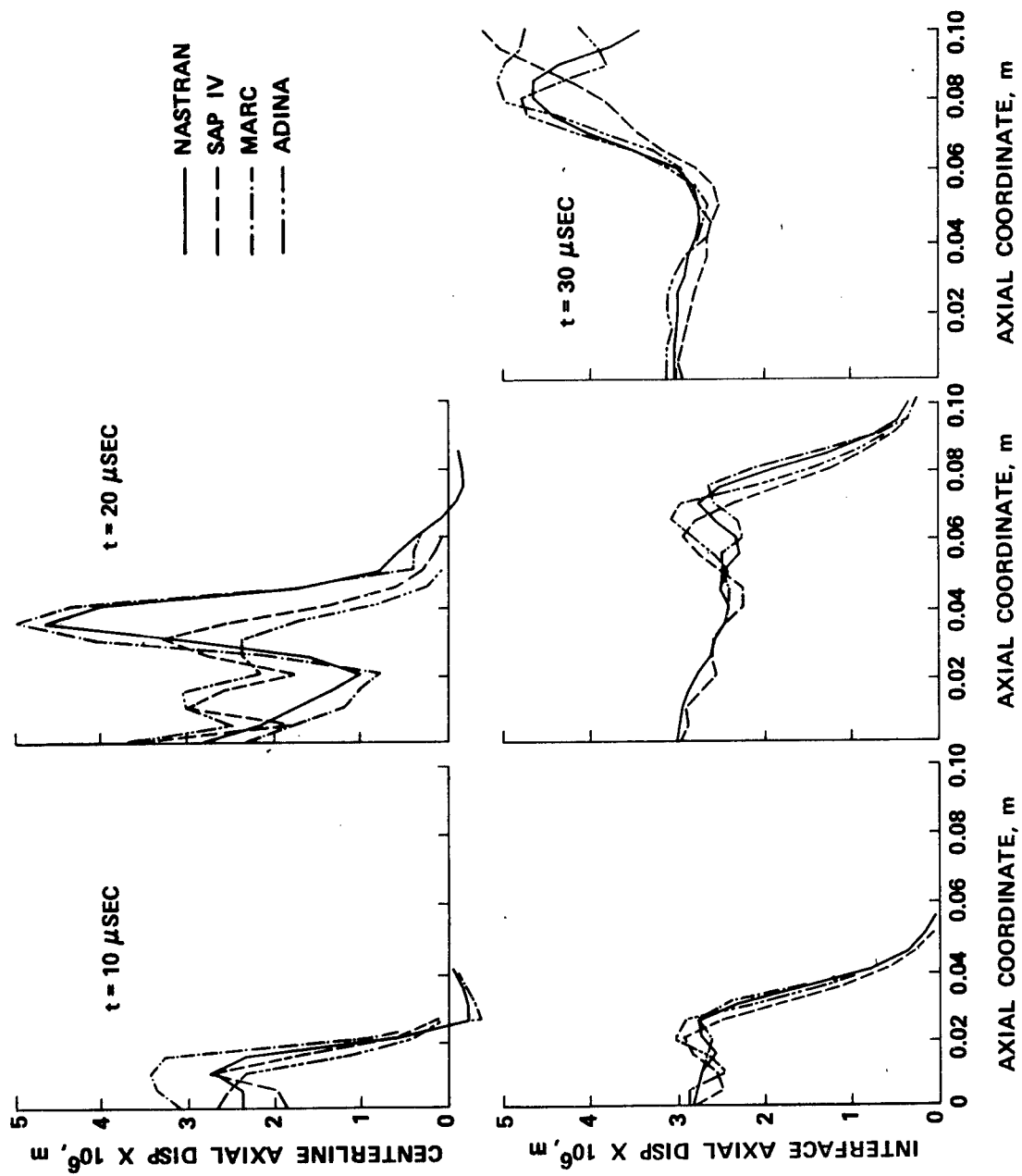


FIGURE 9. Comparison of Linear Analyses for 80-Element Cylinder Impact.

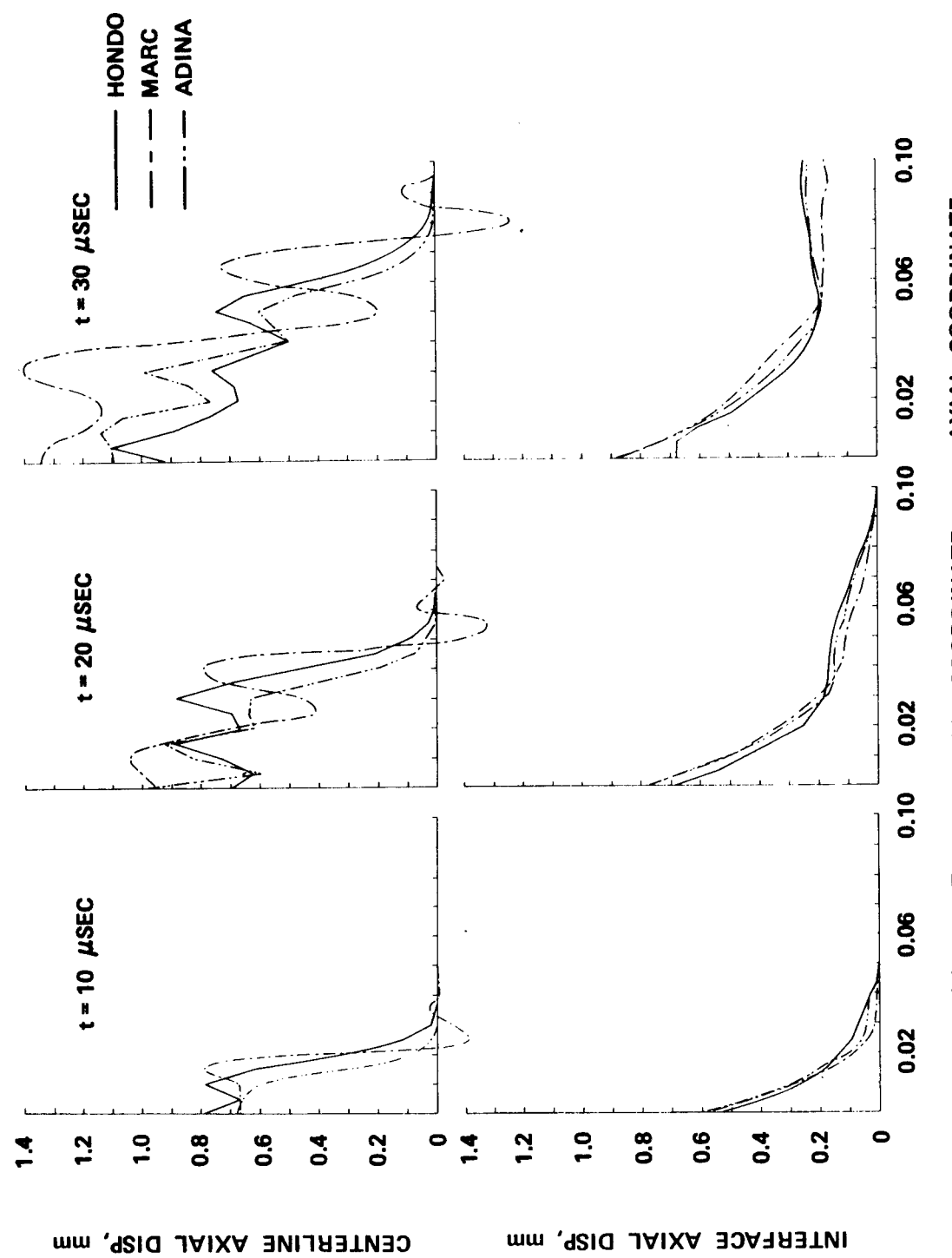


FIGURE 10. Comparison of Nonlinear Analyses for 80-Element Cylinder Impact.

Within each load case all of the programs predict similar axial displacements on the case-explosive interface. Agreement on the centerline displacements is not as good and the differences between the solutions increase with increasing time.

Cylinder Impact. Rather than the half sine pressure pulse that was used to compare codes, impact loading can be represented as an initial velocity condition. Normal end-on impact with a rigid wall requires a uniform axial initial velocity of the cylinder together with zero displacement at the impacting end. NASTRAN was used to obtain the early time response of the model described in Figure 8. Both stresses and displacements were output for times up to 80  $\mu$ sec after impact. Typical axial and circumferential strain histories on the case-explosive interface, and on the centerline are shown in Figures 11 through 13, respectively.

In Figure 11 a compressive wave is observed to be traveling along the length of the cylinder at approximately 5  $\text{mm}/\mu\text{sec}$ . It takes about 20  $\mu\text{sec}$  for the wave to traverse the 100-mm-long cylinder. A reflected wave from the free end of the cylinder does not completely relieve the strains because of interactions between the case and the explosive core. Circumferential strains in the case (see Figure 12) are caused by both the Poisson effect and interface pressures. In this relatively thin case, interface pressures predominate. Consequently, the circumferential strains travel at a slower speed, corresponding to the wave propagation speed in the less rigid explosive material.

The strain history on the centerline of the explosive is less smooth than that on the case (Figure 13). The explosive, being less rigid than the case, is similar to a fluid. In addition to an irrotational wave, it responds to the wall motion. The apparent wave speed of 3  $\text{mm}/\mu\text{sec}$  is somewhat faster than the irrotational wave speed (2.4  $\text{mm}/\mu\text{sec}$ ).

Calculated strains can be compared with predictions based on a one-dimensional wave propagation theory. In the explosive, plane strain should predominate. The corresponding stress, based on quantities from Table 2 is

$$\sigma_{zz}/V = \rho C_1 = 4.3 \times 10^6 \text{ Pa sec/m}$$

where  $V$  is the impact velocity. For the steel case, a plane stress solution yields

$$\sigma_{zz}/V = \rho C_r = 39.4 \times 10^6 \text{ Pa sec/m}$$

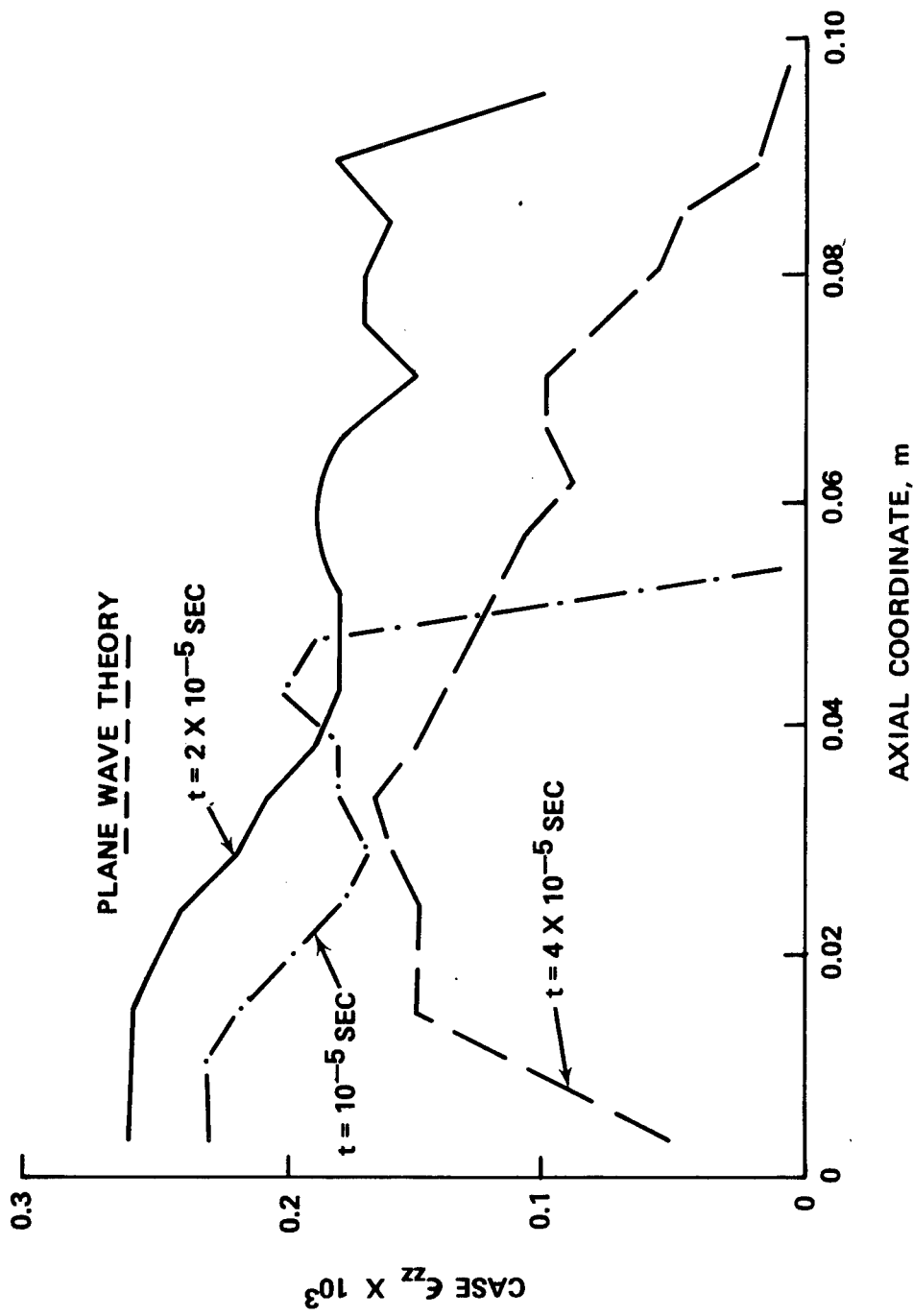


FIGURE 11. Cylinder Impact With Rigid Wall ( $\Delta t = 0.5 \times 10^{-6}$  sec,  $r/R = 1/10$ ).

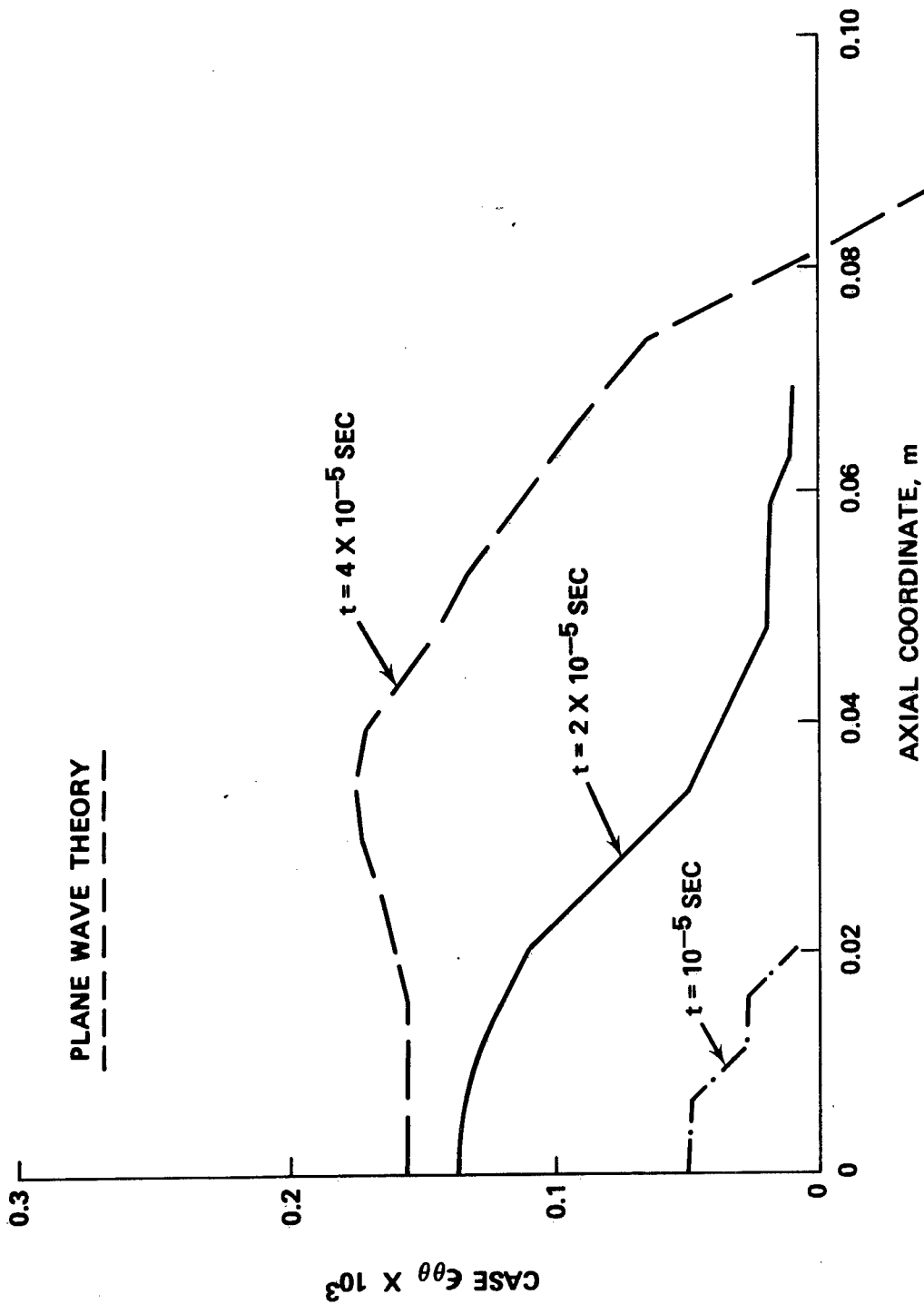


FIGURE 12. Cylinder Impact With Rigid Wall ( $\Delta t = 0.5 \times 10^{-6}$  sec,  $r/R = 1/10$ ).

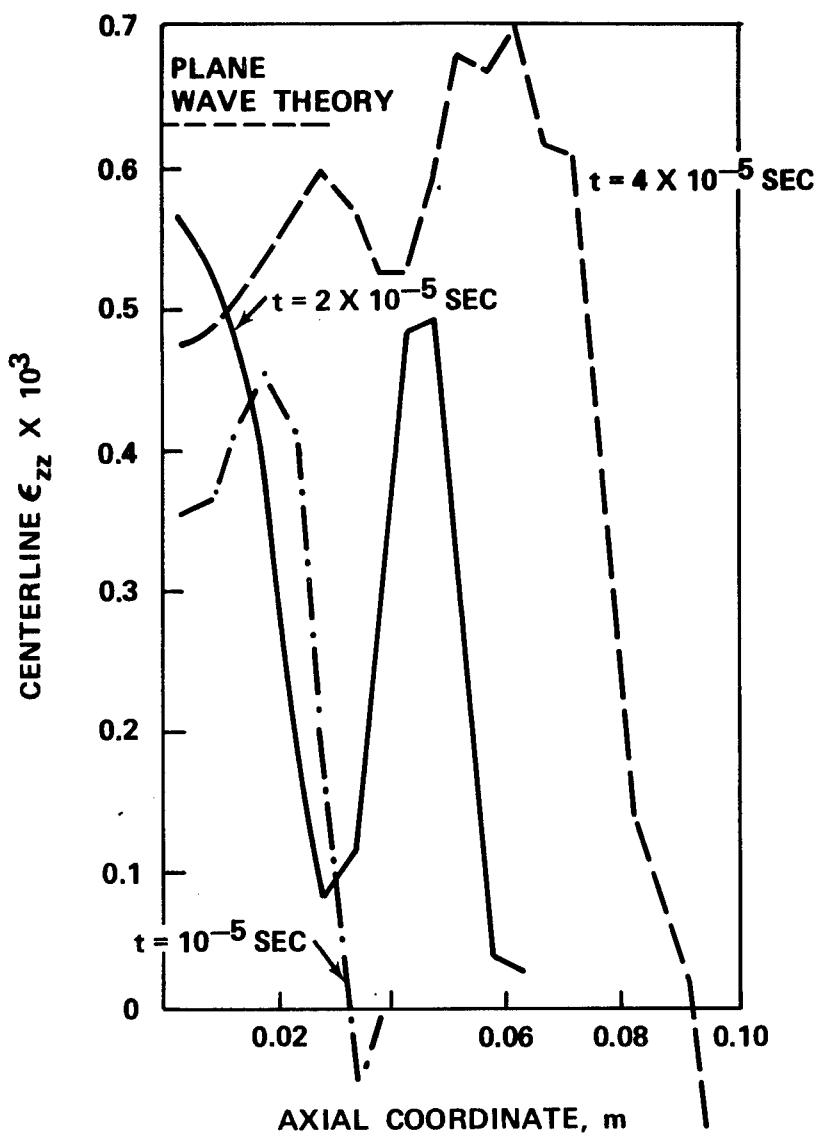


FIGURE 13. Impact With Rigid Wall at 1 m/sec  
 $(\Delta t = 0.5 \times 10^{-6}$  sec,  $r/R = 1/10)$ .

In thin cylinders, the hoop stress caused by hydrostatic pressure from the explosive would be

$$\sigma_{\theta\theta}/V = \rho C_1 R/T = 43 \times 10^6 \text{ Pa sec/m} \quad \text{for } R/T = 10$$

Where  $R$  is the cylinder diameter and  $T$  is the case thickness. Corresponding strains are shown in Figures 11-13. Generally, maximum stresses are close to the plane wave values and occur near the impacted end.

Failure Analysis. Normal impact of an explosive-filled cylinder with a rigid wall can result in failure by breakup of the case, by explosive deflagration, or by detonation of the explosive. Case breakup and deflagration are stress-dependent failure modes while detonation is dependent on stress history in the explosive. An analysis of stresses in elastic cylinders has been conducted to determine how the minimum impact speed for failure depends on the wall thickness. Surprisingly, the lowest predicted speed at which yield occurs in a steel case and deflagration occurs in the explosive core are both only weakly dependent on case thickness.

The finite element analysis described in the previous section provides stresses in each element used to represent the body. From an average taken from a cross section near the impacted end, impact stresses are obtained for comparison with the yield and deflagration failure criterion. Detonation of the explosive is not considered since we are looking for the lowest impact speed at which failure occurs.\* Both plastic yielding of the steel cylinder and deflagration of the explosive are considered. A 5-Kbar pressure deflagration condition has been assumed. The resulting minimum impact velocities for failure are shown in Figure 14. These failure speeds are surprisingly insensitive to the wall thickness. There is also relatively little effect of the cylinder end conditions on the failure speeds. End conditions considered were that the impact end of the cylinder was either free to expand radially or was fixed radially. These cases simulate impact of open and closed ended warheads, respectively.

#### CONICAL WARHEAD

One advantage of the finite element procedure is its ability to handle non-simple geometries. To illustrate this capability, another

---

\* An energy density failure criterion is appropriate for detonation. An example of a problem for application of this criterion would be determining the maximum plate thickness that could be penetrated at some impact speed without warhead detonation.

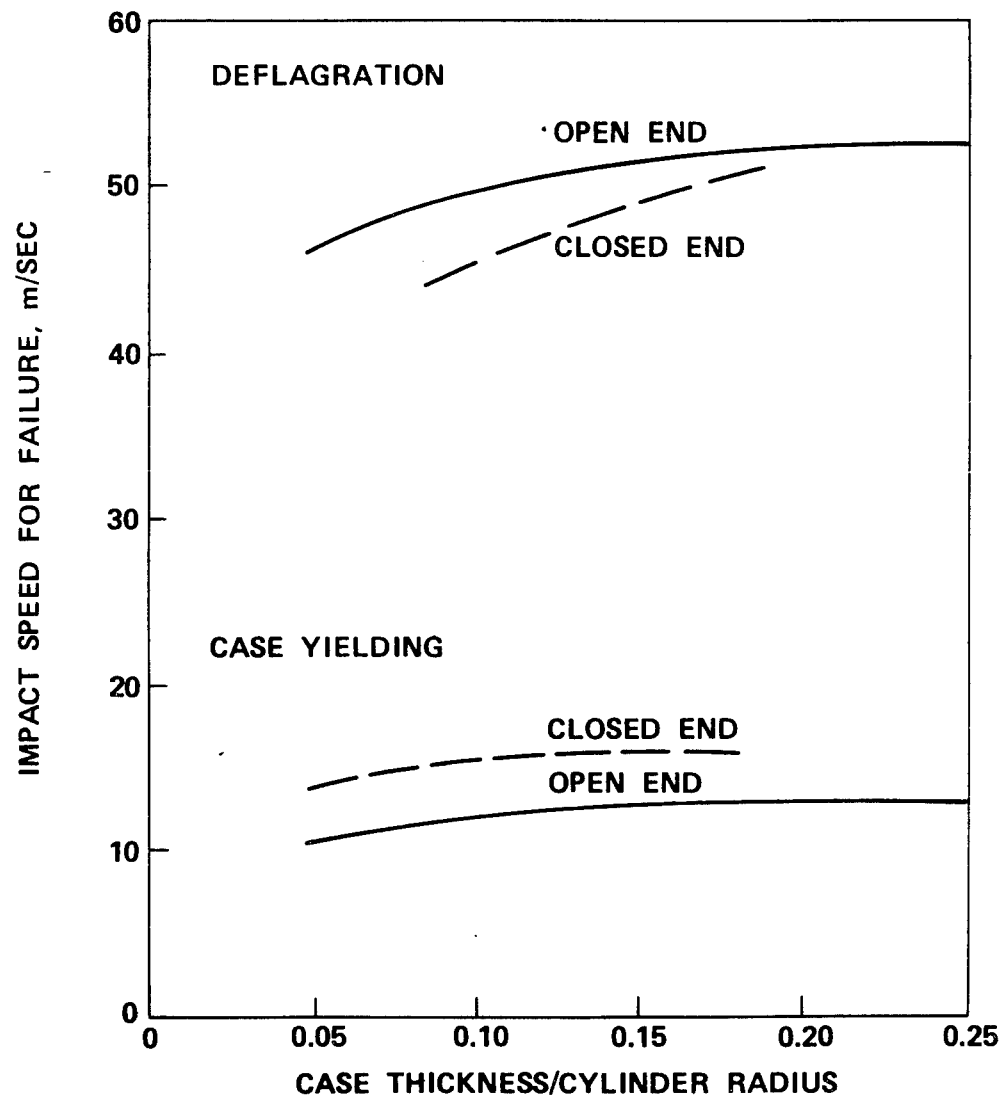


FIGURE 14. Effect of Wall Thickness on Failure Speed.

warhead configuration consisting of an explosive-filled conical steel case with linearly varying thickness was considered. Two different material characterizations were used. In the first, both the case and explosive were assumed to behave elastically. In the second, the explosive was assumed to behave elastically, but the case was treated as an elastic, perfectly plastic material. As in the concentric cylinder problem, the loading consisted of a half sine pressure pulse at one end. The other end was built in.

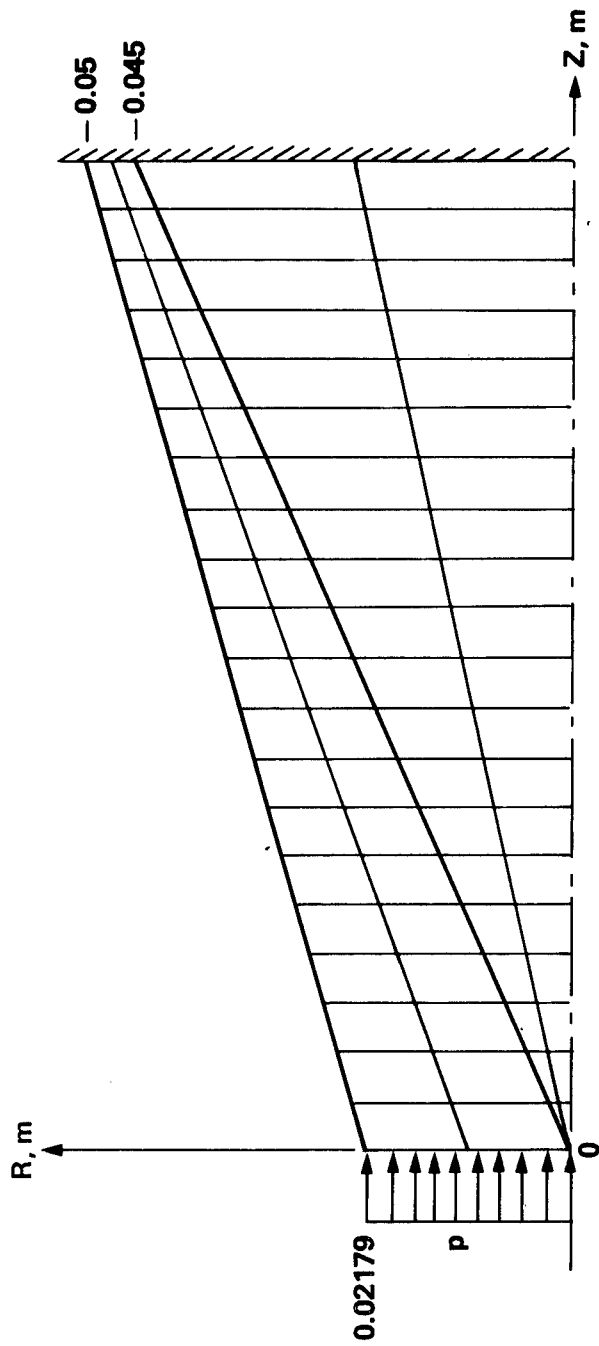
Several different model representations were used in the runs made with the various programs. For the NASTRAN and SAP IV runs, four layers of axisymmetric elements were used; two to represent the case, and two to represent the explosive. There were 20 elements down the length of the warhead in each layer. The integration step size was selected as one-twentieth of the pulse length. The geometry and properties of this configuration are shown in Figure 15. In the ADINA runs, six layers (three for the case, and three for the explosive) were used. The HONDO, SHELL SHOCK and TOODY-IIA runs were made with variable sized meshes with many small elements near the loaded end and fewer relatively large elements at the other end.\*

The results are summarized in Figures 16-19, which are plots, respectively, of centerline displacement, interface axial displacement, case axial stress near the interface, and case radial stress near the interface versus axial distance from the loaded end at 10  $\mu$ sec. Separate plots for the linear and nonlinear runs are given in each figure. It is obvious that there are considerable differences in the results for the various programs, due in part to differences in the programs themselves (different elements, integration schemes, etc.), and also to differences in the model representations used. Nevertheless, the gross behavior of the various solutions is reasonably similar. This is especially true for the displacements. There is more variation in the stress results. As would be expected, the nonlinear plots show larger peak displacements and smaller maximum stresses than the linear ones.

Although the results for the various programs at 10  $\mu$ sec are in reasonable agreement with each other (and probably with the "true" solution, if one were available), agreement at later times is not as good. Figure 20 is a series of plots of centerline displacement versus axial distance from the loaded end at 10  $\mu$ sec intervals up to 80  $\mu$ sec for the NASTRAN and SAP IV runs. After about 40  $\mu$ sec, it is difficult to recognize the two solutions as applying to the same problem. This indicates

---

\* The solutions to this problem using SHELL SHOCK, HONDO, and TOODY-IIA were obtained by Kaman Sciences Corp. SHELL SHOCK and TOODY-IIA are not available on the NWC UNIVAC 1110 at the present time.



$$P = 3.212 \times 10^9 \sin [(2\pi \times 10^5)t] \text{ Pa}, 0 < t < 5 \times 10^{-6} \text{ SEC}$$

$$P = 0, 5 \times 10^{-6} < t$$

	CASE	EXPLOSIVE
$E$	$2 \times 10^{11} \text{ Pa}$	$6.9 \times 10^9 \text{ Pa}$
$\nu$	0.3	0.34
$\rho$	$7800 \text{ Kg/m}^3$	$1800 \text{ Kg/m}^3$
$\sigma_y$	$10.35 \times 10^8 \text{ Pa}$	—

FIGURE 15. Geometry and Properties for Conical Warhead Problem.

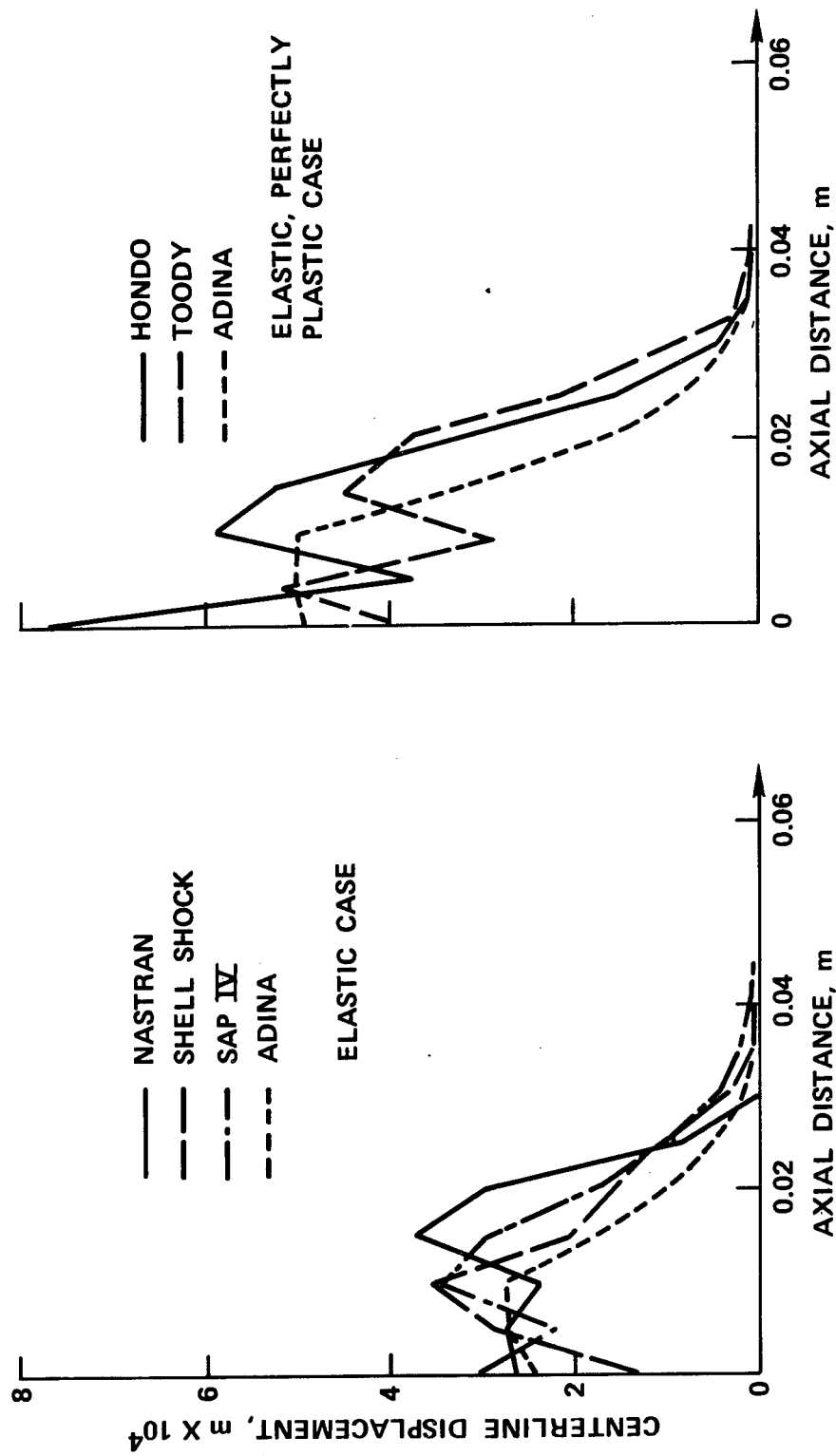


FIGURE 16. Conical Warhead Impact, Interface Axial Displacement Versus Axial Distance,  
 $P_0 = 3.212 \times 10^9$  Pa,  $t = 10$   $\mu$ sec.

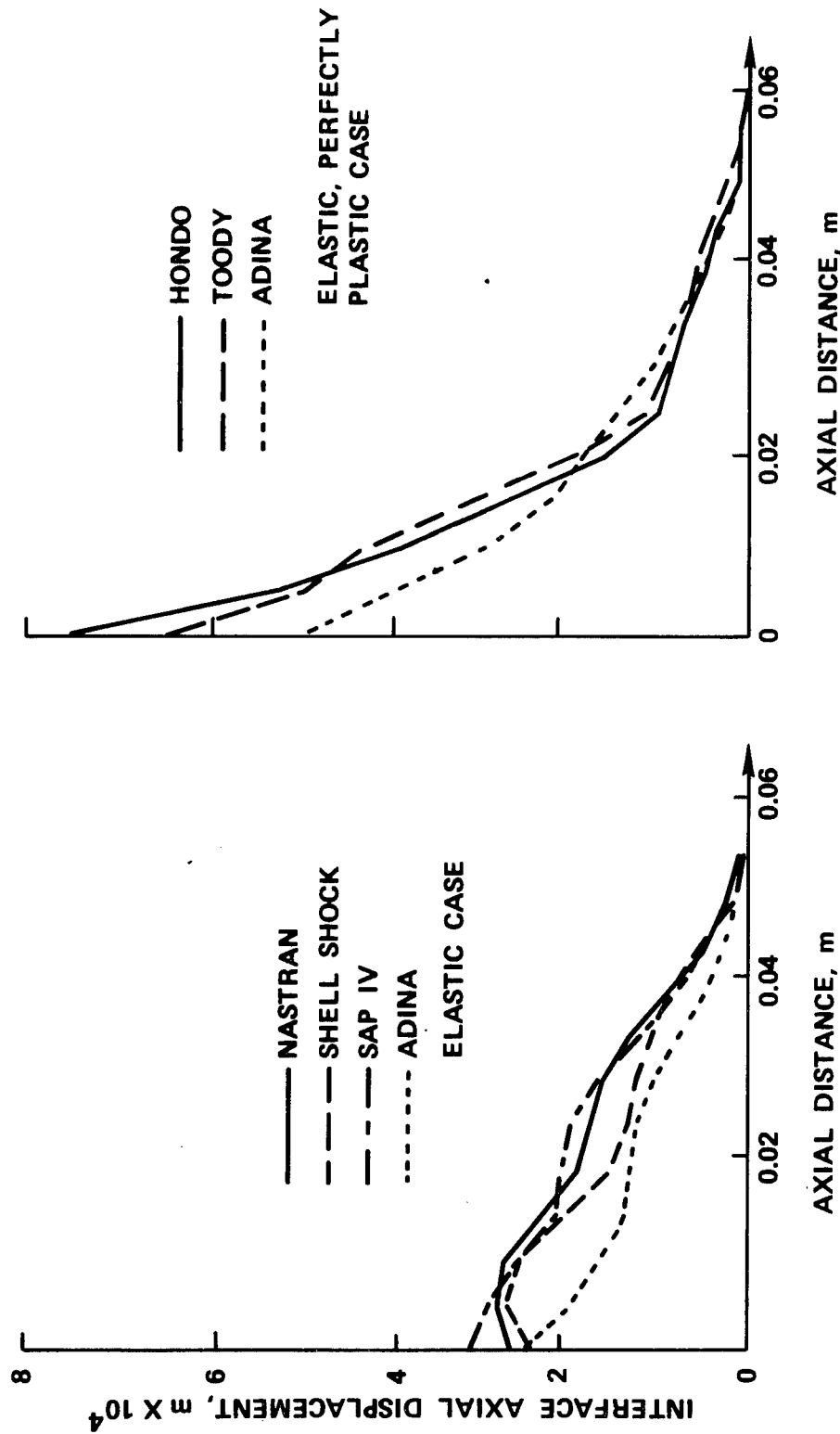


FIGURE 17. Conical Warhead Impact, Interface Axial Displacement Versus Axial Distance,  $p_0 = 3.212 \times 10^9$  Pa,  $t = 10$   $\mu$ sec.

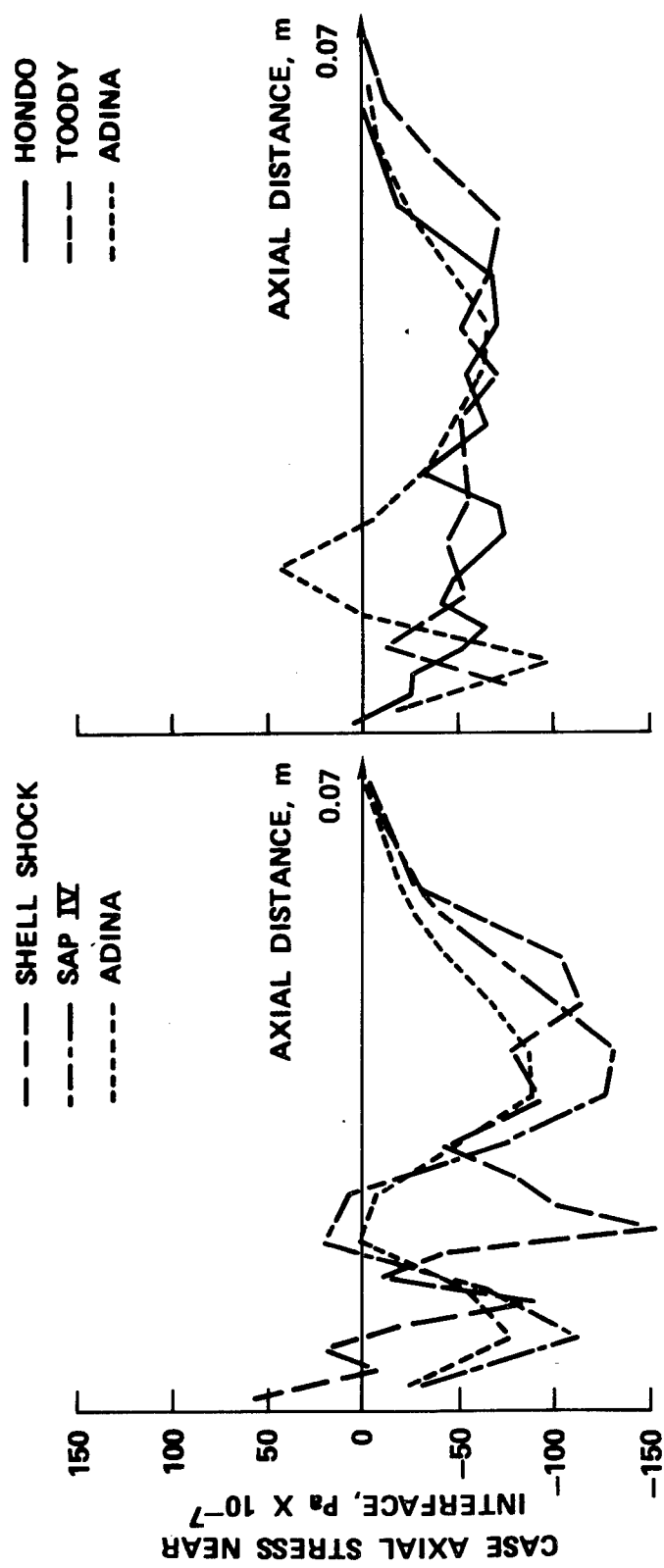


FIGURE 18. Conical Warhead Impact, Case Axial Stress Near Interface Versus Axial Distance,  $P_0 = 3.212 \times 10^9$  Pa,  $t = 10$   $\mu$ sec.

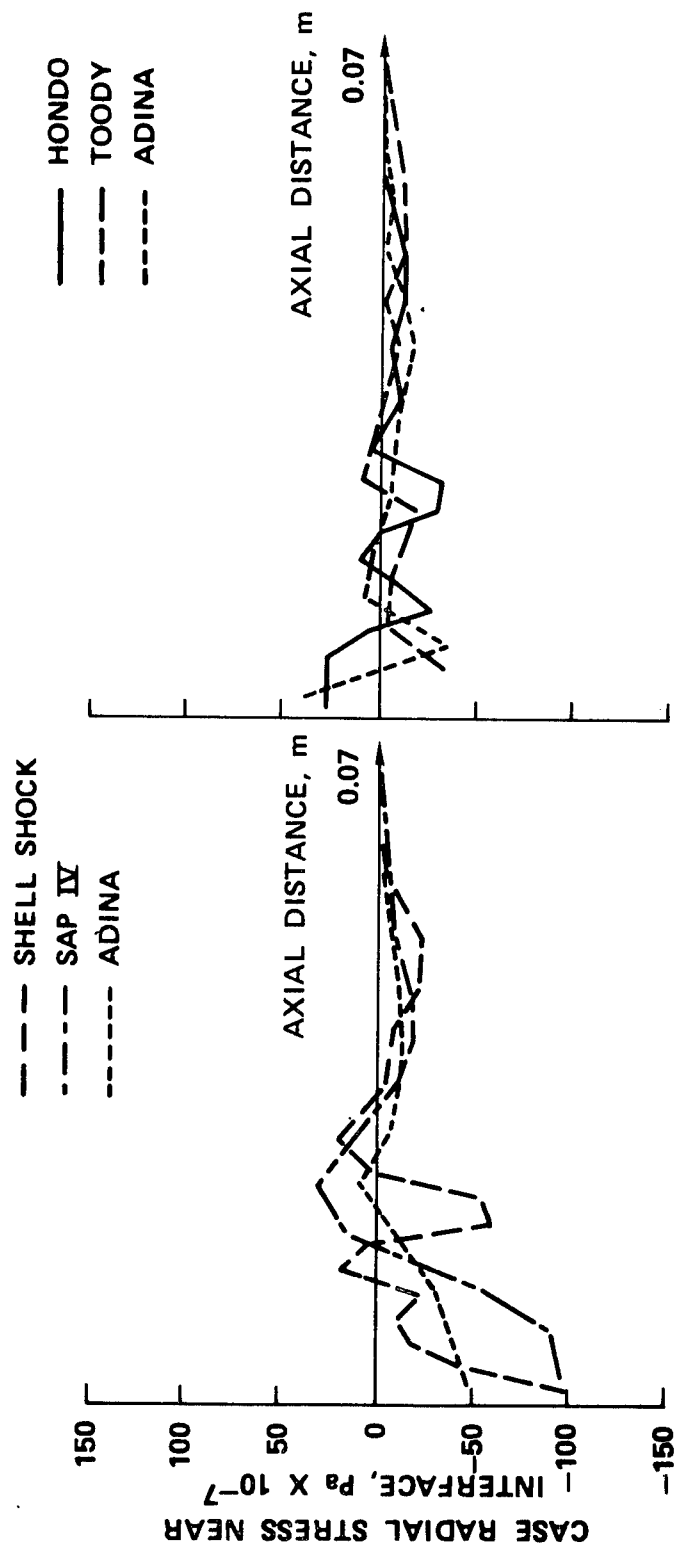


FIGURE 19. Conical Warhead Impact, Case Radial Stress Near Interface Versus Axial Distance,  $P_0 = 3.212 \times 10^9 \text{ Pa}$ ,  $t = 10 \text{ usec.}$

that the model used is not sufficiently detailed to obtain accurate long-term solutions. A finer grid and small time steps would be required to produce such solutions.

Breakdown of the conical warhead solution is more rapid than solution breakdown in the problems previously treated. This is probably due to the fact that in the previous problems the primary effect of the pressure load is to produce longitudinal stress waves which travel down the length of the cylinder. Transverse dispersion effects are of only secondary importance. In the conical warhead problem, however, due to the greater case thickness and conical geometry, transverse waves produced by reflection from the conical surfaces will make an important contribution right from the start and can be expected to cause differences between the solutions at earlier times.

#### SPHERICAL CAVITY

There are surprisingly few dynamic plasticity problems involving more than a one-dimensional state of stress for which analytic solutions are available. Even such a simple-appearing problem as that of an infinite elastic, perfectly plastic medium containing a spherical cavity subjected to a step pressure cannot be solved completely by analytic means. However, an analytic solution to this problem can be obtained for short times, and a good numerical solution can be generated for larger times. It was decided, therefore, to use this problem to test the relative efficiency and accuracy of some of the nonlinear structural analysis programs.

The spherical cavity problem for an elastic, perfectly plastic medium was discussed at length in the survey article by Hopkins.<sup>6</sup> He gives a formal solution in terms of a set of ordinary differential equations involving the plastic wave functions,  $H$  and  $K$ , the elastic wave function,  $F$ , and the speed of the elastic-plastic boundary,  $b$ .

Application of a step pressure at the cavity radius causes an elastic wave to propagate outward into the medium with a constant speed,  $c_e$ . If the pressure is greater than that required to initiate yielding, then the elastic wave will be followed by a plastic wave traveling at a slower but constant speed,  $b = c_p$ . There will be a discontinuity in stress across the boundary between the elastic and plastic regions. As time increases, the magnitude of this discontinuity will decrease until at

---

<sup>6</sup> H. G. Hopkins. *Progress in Solid Mechanics*, North-Holland Publishing Co., Amsterdam, Vol. 1, Chapter III, 1960, pp. 83-164.

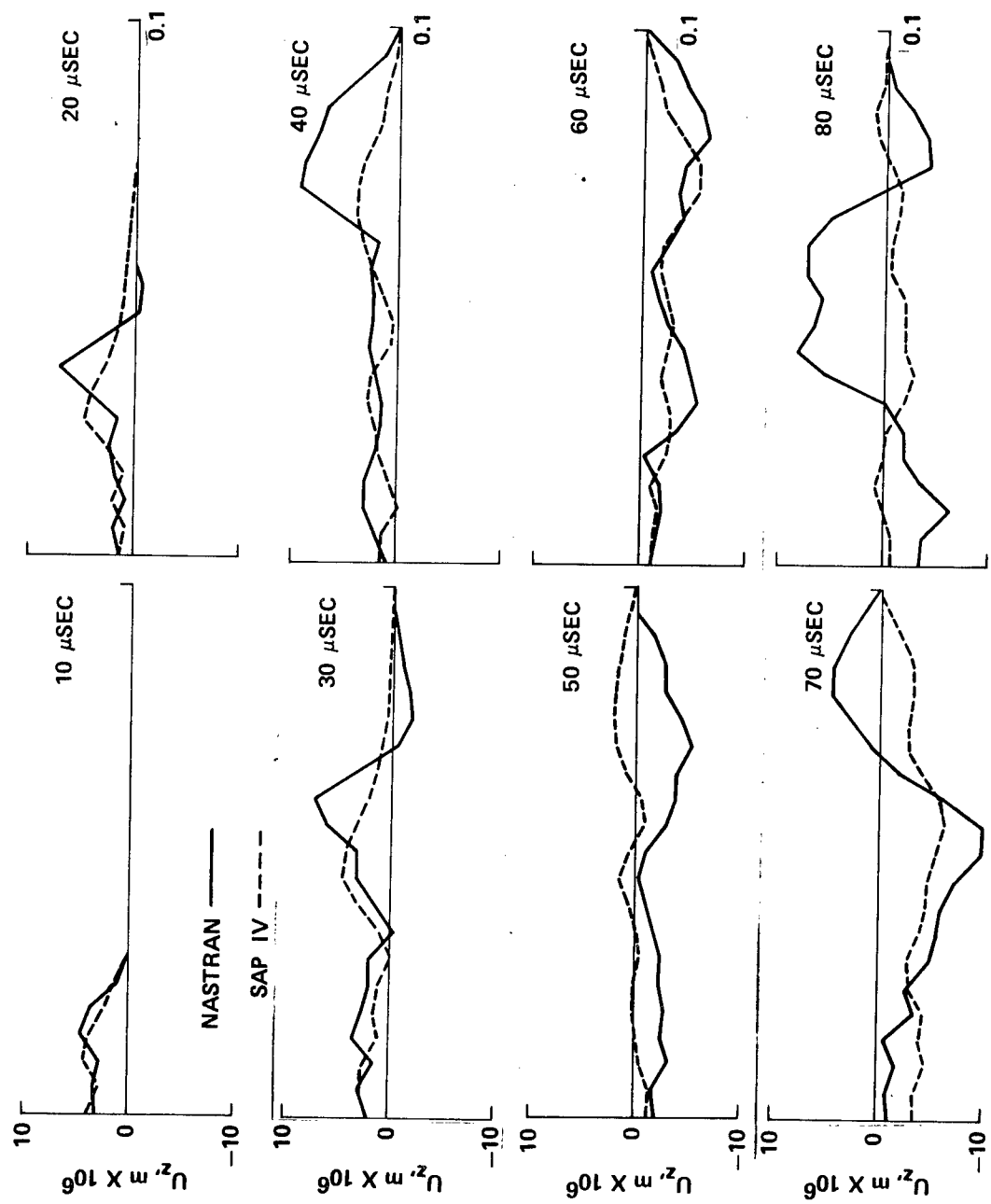


FIGURE 20. Conical Warhead Problem. Plots of centerline displacement versus axial distance at selected times for NASTRAN and SAP IV runs.

some time,  $t_m$ , it will disappear entirely. Up to this time an analytic solution to the problem can be obtained by integration of the governing equations given by Hopkins.

For times greater than  $t_m$ , the character of the solution changes somewhat. The speed of the elastic-plastic boundary no longer remains constant, but begins to decrease. Because the boundary speed is no longer a known constant, an additional unknown is introduced into the problem. Moreover, because this unknown enters into the governing equations in a nonlinear way, an analytic solution is no longer possible. However, the governing equations can still be integrated numerically using an iterative procedure to eliminate the stress discontinuity between the elastic and plastic regions. Though only approximate, this iterative solution can be expected to be considerably more accurate than finite element solutions because it takes into account the possible presence of discontinuities at the elastic wave front and the elastic-plastic boundary.

This solution was used as a standard of comparison for finite element results obtained using ADINA and HONDO. The spherical cavity problem is one-dimensional. Unfortunately, none of the structural analysis programs considered here have one-dimensional spherical elements in their libraries. Consequently, it was necessary to use a two-dimensional finite element model. A narrow conical sliver of material with the apex of the cone coinciding with the center of the cavity was selected for analysis. This conical sliver was modeled using axisymmetric elements. Because of symmetry, points on the side of the cone can only move radially outward. This boundary condition cannot be imposed directly using program ADINA. It was necessary, therefore, in the ADINA runs to attach very long, stiff and massless truss elements perpendicular to the side at these points to prevent radial motion. The model geometry is shown in Figure 21.

A comparison of results obtained using ADINA and HONDO with the analytic-numeric solution is given in Figure 22, which is a series of plots of radial stress versus radial distance at selected times. Agreement between the HONDO results and the "exact" solution is quite good, even in the vicinity of the stress discontinuities, which the program does its best to represent. The ADINA results are not as satisfactory. Not only are there greater errors near the discontinuities, but fairly substantial oscillations about the true solution are present. Hopefully, the new version of ADINA due to be released soon will provide better results for this problem.

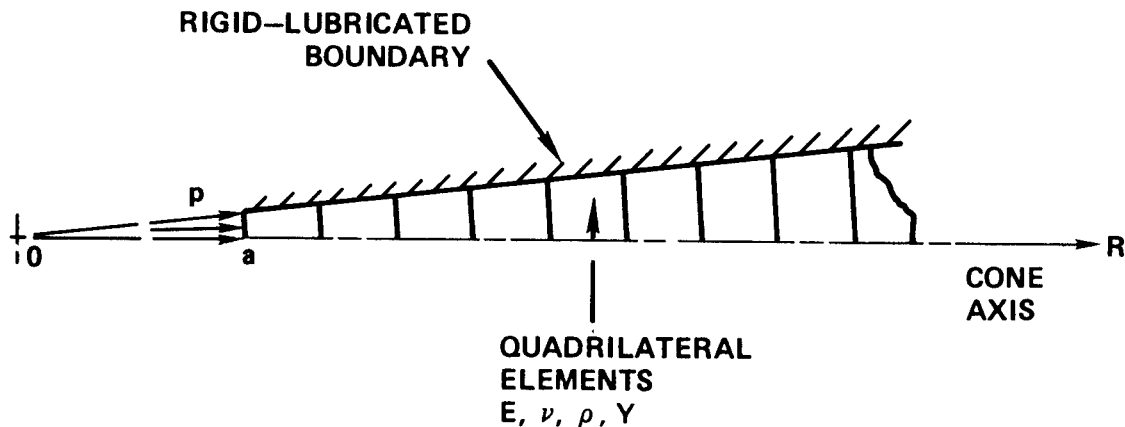


FIGURE 21. Geometry of Spherical Cavity Model.

### CONCLUSIONS

Based on the foregoing results, the following conclusions can be drawn regarding the usefulness of finite element structural analysis programs for warhead design work.

### ACCURACY

For simple geometries where the wave propagation is essentially longitudinal (e.g., the rod problems and the Bertholf cylinder) reasonably accurate solutions were obtained with the mesh sizes and time steps used. The results remained adequate for the time required for a wave to travel the length of the cylinder and return to the loaded end. In the case of the more geometrically complicated conical warhead, the results became essentially meaningless before the wave had traveled even the length of the warhead. Successful analysis of this problem for a longer period of time would require a much finer model and smaller time steps. The cost of such an analysis might become extremely high.

It is difficult to assess the relative accuracy of the various programs in quantitative terms because of a lack of exact solutions (except for the very simple problems) with which to compare the results. Clearly, the version of ADINA implemented at NWC was not as accurate as HONDO in the problems to which they were both applied. On the other hand, while there were differences in the results obtained using the other programs, no one program appeared to be significantly more or less accurate than the others.

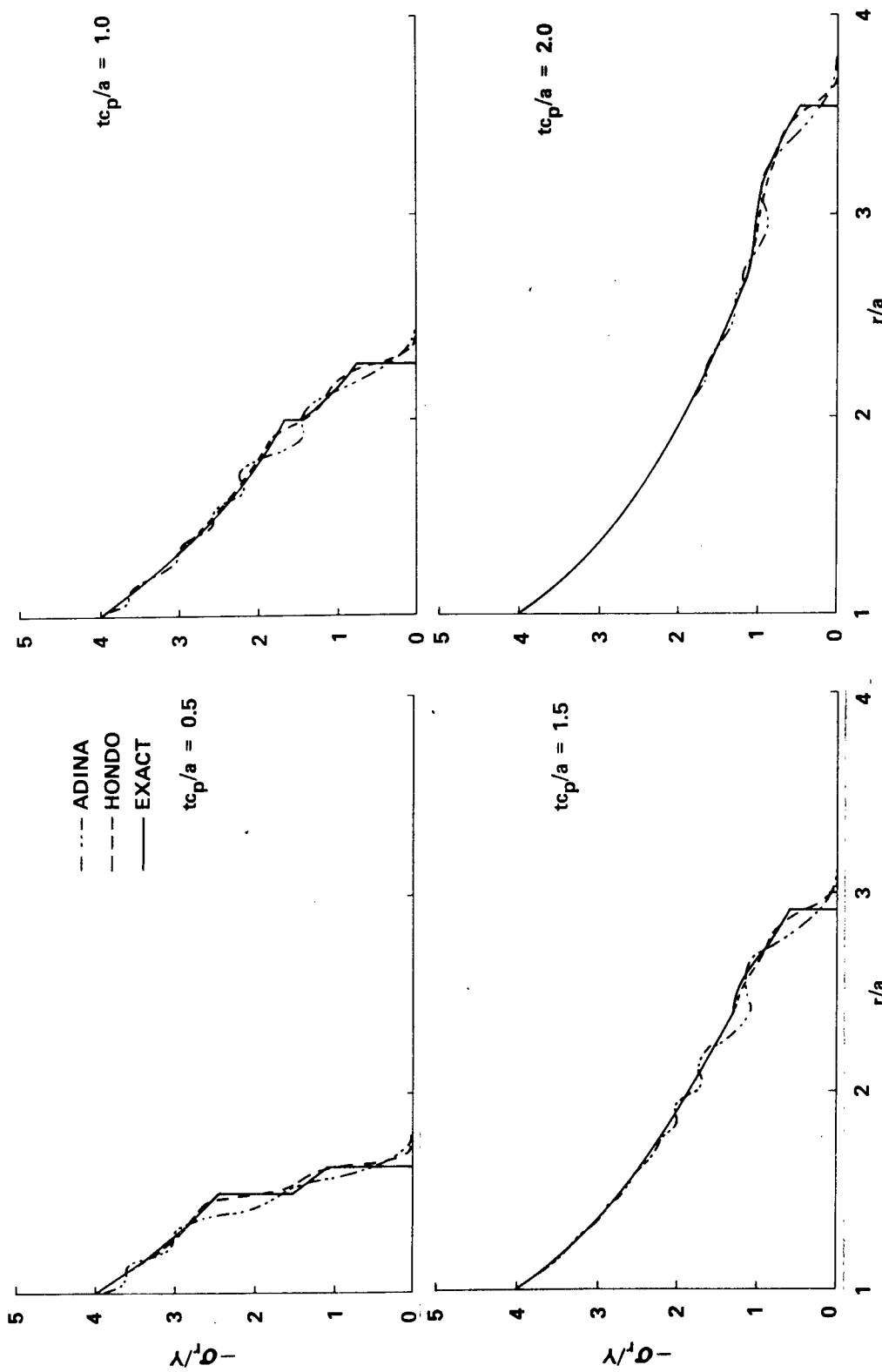


FIGURE 22. Spherical Cavity Problem. Radial stress versus radial distance at selected times.

#### TIME AND COST

The CAU times and costs on the NWC UNIVAC 1110 system for the various problem solutions are given in Table 4. For some of the runs not made at NWC, times were converted to equivalent UNIVAC 1110 times. The table shows that, by and large, those programs with more features and capabilities take longer to solve problems. This can be seen by comparing the NASTRAN and SAP IV solution times for those problems they were both used to solve. The Bertholf cylinder problem, for example, required 596 CAU seconds and cost \$255 using NASTRAN—compared to only 182 seconds and \$120 using SAP IV. Because of its smaller size (number of FORTRAN statements), SAP IV was able to solve some problems in-core without the use of external storage. It is likely that for extremely large problems, which neither program could solve in-core, NASTRAN would come into its own, so to speak, and the cost and time differences between the two would largely disappear. Surprisingly, MARC, which has a reputation for being slow, actually required less CAU time than did NASTRAN to solve the concentric cylinder problem. HONDO, which is an in-core solver, was by far the fastest of the nonlinear programs. For the spherical cavity problem, HONDO required only 55 CAU seconds and \$14—compared to 557 seconds and \$158 for ADINA.

#### EASE OF USE

For the most part, those programs requiring the least amount of input tend to be the easiest to use. Less input means less time spent on problem preparation and less likelihood of mistakes. From this standpoint, it would appear that SAP IV should be the program of choice for three-dimensional linear elastic problems and that HONDO should be used for linear and nonlinear problems involving axisymmetric solids. Use of other programs is justified only when their special capabilities (such as the fluid elements available in NASTRAN) permit the solution of problems not tractable with the other programs.

#### EASE OF LEARNING

The difficulty involved in learning to use a program depends in large measure on the complexity of the program itself and on the amount of input required. Hence, programs that are easy to use tend to be easy to learn how to use. HONDO, NONSAP and ADINA are offshoots of SAP IV. A designer or analyst familiar with the format and nomenclature used in SAP IV can expect to learn to use these other programs relatively quickly. NASTRAN is especially difficult to learn because the user's manual is cumbersome and hard to read. However, once the manual has been mastered, use of the program is not difficult.

TABLE 4. Cost and Time Comparison for the Various Runs.

Problem	Degrees of freedom	Bandwidth	Number of time steps	Program	CAU time seconds	Cost, dollars
1-D rod, elastic, half sine pressure pulse	20	2	100	NASTRAN SAP IV	19 2	21 3
	100	2	200	SAP IV	7	7
1-D rod, elastic-plastic, step pressure	400	8	236	HONDO	57	14
Bertholf cylinder, elastic, step pressure	640	25	80	NASTRAN SAP IV	596 182	255 120
Bertholf cylinder, elastic-plastic, impact	364	18	52	HONDO	33	12
Concentric cylindrical warhead, elastic, half sine pressure pulse	110	14	30	NASTRAN NONSAF (ln)	60 3	
	210	14	30	NASTRAN SAP IV NONSAF (ln)	190 10 4	
	546	30	30	SAP IV	44	
Concentric cylindrical warhead, elastic-plastic, half sine pressure pulse	110	14	30	NONSAF	41	
	210	14	30	NONSAF MARC ADINA HONDO	75 175 150 8	116 3
	510	21	160	SAP IV	223	145
Conical warhead, elastic half sine pressure pulse	176	13	80	NASTRAN SAP IV	155 12	81 7
Conical warhead, elastic, 1 m/s impact	176	13	20	NASTRAN	95	52
Spherical cavity, elastic, step pressure	302	6	88	SAP IV ADINA (ln)	15 19	11 13
	404	8	170	HONDO (ln)	30	9
Spherical cavity, elastic-plastic, step pressure	452	6	100	ADINA	557	158
	604	8	150	HONDO	55	14

## SUMMARY

This report has been concerned with the application of general purpose finite element structural analysis programs to warhead design work. A number of linear and nonlinear codes were described. These were applied to the solution of impact-type problems of varying complexity. Based on the results obtained, the various programs were compared with regard to accuracy, time and cost, ease of learning, and ease of use. Considering only those programs currently available at NWC, it would appear that SAP IV is the preferred program for linear elastic problems, while HONDO is best suited for nonlinear problems involving axial symmetry. Because of accuracy problems, the current version of ADINA should be used with caution.

INITIAL DISTRIBUTION

1 Director of Navy Laboratories  
13 Naval Air Systems Command  
    AIR-30212 (2)  
    AIR-350 (1)  
    AIR-350D (1)  
    AIR-5108 (1)  
    AIR-5321 (1)  
    AIR-5323 (2)  
    AIR-5324 (1)  
    AIR-53242 (1)  
    AIR-533 (1)  
    AIR-954 (2)  
5 Chief of Naval Operations  
    OP-03EG (2)  
    OP-05 (1)  
    OP-098 (1)  
    OP-55 (1)  
2 Chief of Naval Material  
    MAT-03 (1)  
    MAT-03PB (1)  
7 Naval Sea Systems Command  
    SEA-033 (5)  
    SEA-09G32 (2)  
4 Chief of Naval Research, Arlington  
    ONR-102 (1)  
    ONR-429 (1)  
    ONR-461 (1)  
    ONR-473 (1)  
1 Air Test and Evaluation Squadron 5  
1 Fleet Anti-Air Warfare Training Center, San Diego  
1 Marine Air Base Squadron 32, Beaufort  
1 Marine Corps Air Station, Beaufort  
1 Naval Air Engineering Center, Lakehurst  
1 Naval Air Force, Atlantic Fleet  
2 Naval Air Force, Pacific Fleet  
1 Naval Air Station, North Island  
2 Naval Air Test Center (CT-176), Patuxent River (Aeronautical Publications Library)  
1 Naval Avionics Facility, Indianapolis (Technical Library)  
1 Naval Explosive Ordnance Disposal Facility, Indian Head

1 Naval Ocean Systems Center, San Diego (Code 1311)  
1 Naval Ordnance Station, Indian Head (Technical Library)  
1 Naval Postgraduate School, Monterey  
1 Naval Ship Research and Development Center, Bethesda  
5 Naval Surface Weapons Center, White Oak  
    WR-13, R. Liddiard (1)  
    Dr. S. Jacobs (1)  
    J. Erkman (1)  
    Guided Missile Warhead Section (1)  
    Technical Library (1)  
1 Office of Naval Research Branch Office, Chicago  
1 Office of Naval Research Branch Office, Pasadena  
1 Operational Test and Evaluation Force  
1 Pacific Missile Test Center, Point Mugu (Technical Library)  
1 Army Armament Command, Rock Island (SMUAP-MI-T, Technical Library)  
1 Aberdeen Proving Ground (Development and Proof Services)  
4 Army Armament Research & Development Center  
    SARPA-AD-D-A-3, J. Pentel (1)  
    Technical Library (3)  
2 Army Ballistics Research Laboratories, Aberdeen Proving Ground  
    AMXBR-T, Detonation Branch (1)  
    AMXBR-XA-FI (1)  
1 Army Material Systems Analysis Agency, Aberdeen Proving Ground  
    (J. Sperrazza)  
1 Army Research Office, Durham  
1 Harry Diamond Laboratories (Technical Library)  
1 Radford Army Ammunition Plant  
1 Redstone Arsenal (Rocket Development Laboratory, Test and  
    Evaluation Branch)  
1 Rock Island Arsenal  
1 White Sands Missile Range (STEWS-AD-L)  
1 Yuma Proving Grounds (STEYT-GTE, M&W Branch)  
1 Tactical Air Command, Langley Air Force Base (TPL-RQD-M)  
1 Air University Library, Maxwell Air Force Base  
3 Armament Development & Test Center, Eglin Air Force Base  
2 57th Fighter Weapons Wing, Nellis Air Force Base  
    FWOA (1)  
    FWOT (1)  
3 Tactical Fighter Weapons Center, Nellis Air Force Base  
    COA (1)  
    CRCD (1)  
    CTE (1)  
12 Defense Documentation Center  
1 Defense Nuclear Agency (Shock Physics Directorate)  
1 Weapons Systems Evaluation Group  
1 Lewis Research Center  
2 Allegany Ballistics Laboratory, Cumberland, MD

2 Applied Physics Laboratory, JHU, Laurel, MD (Document Library)  
1 Arthur D. Little, Inc., Cambridge, MA (W. H. Varley)  
2 Chemical Propulsion Information Agency, Applied Physics Laboratory,  
Laurel, MD  
1 IIT Research Institute, Chicago, IL (Document Librarian for  
Department M)  
1 Jet Propulsion Laboratory, CIT, Pasadena, CA (Technical Library)  
1 Los Alamos Scientific Laboratory, Los Alamos, NM (Reports Library)  
1 Princeton University, Forrestal Campus Library, Princeton, NJ  
1 Stanford Research Institute, Poulter Laboratories, Menlo Park, CA  
1 The Rand Corporation, Santa Monica, CA (Technical Library)  
1 University of California, Lawrence Livermore Laboratory, Livermore, CA  
1 University of Denver, Denver Research Institute, Denver, CO